

AWARD NUMBER: W81XWH-16-1-0448

TITLE: Translational Significance of p53 Loss of Heterozygosity in Breast Cancer

PRINCIPAL INVESTIGATOR: Natalia Marchenko

CONTRACTING ORGANIZATION:

Research Foundation for the State University
Stony Brook, NY 11794

REPORT DATE: Sept 2018

TYPE OF REPORT: Annual

PREPARED FOR: U.S. Army Medical Research and Materiel Command
Fort Detrick, Maryland 21702-5012

DISTRIBUTION STATEMENT: Approved for Public Release;
Distribution Unlimited

The views, opinions and/or findings contained in this report are those of the author(s) and should not be construed as an official Department of the Army position, policy or decision unless so designated by other documentation.

REPORT DOCUMENTATION PAGE

Form Approved
OMB No. 0704-0188

Public reporting burden for this collection of information is estimated to average 1 hour per response, including the time for reviewing instructions, searching existing data sources, gathering and maintaining the data needed, and completing and reviewing this collection of information. Send comments regarding this burden estimate or any other aspect of this collection of information, including suggestions for reducing this burden to Department of Defense, Washington Headquarters Services, Directorate for Information Operations and Reports (0704-0188), 1215 Jefferson Davis Highway, Suite 1204, Arlington, VA 22202-4302. Respondents should be aware that notwithstanding any other provision of law, no person shall be subject to any penalty for failing to comply with a collection of information if it does not display a currently valid OMB control number. **PLEASE DO NOT RETURN YOUR FORM TO THE ABOVE ADDRESS.**

1. REPORT DATE Sept 2018		2. REPORT TYPE Annual		3. DATES COVERED 1 Sep 2017-31 Aug 2018	
4. TITLE AND SUBTITLE Translational Significance of p53 Loss of Heterozygosity in Breast Cancer				5a. CONTRACT NUMBER	
				5b. GRANT NUMBER W81XWH-16-1-0448	
				5c. PROGRAM ELEMENT NUMBER	
6. AUTHOR(S) Natalia Marchenko Email: Natalia.marchenko@stonybrookmedicine.edu				5d. PROJECT NUMBER	
				5e. TASK NUMBER	
				5f. WORK UNIT NUMBER	
7. PERFORMING ORGANIZATION NAME(S) AND ADDRESS(ES) Research Foundation for the State University Stony Brook, NY 11794				8. PERFORMING ORGANIZATION REPORT NUMBER	
9. SPONSORING / MONITORING AGENCY NAME(S) AND ADDRESS(ES) U.S. Army Medical Research and Materiel Command Fort Detrick, Maryland 21702-5012				10. SPONSOR/MONITOR'S ACRONYM(S)	
				11. SPONSOR/MONITOR'S REPORT NUMBER(S)	
12. DISTRIBUTION / AVAILABILITY STATEMENT Approved for Public Release; Distribution Unlimited					
13. SUPPLEMENTARY NOTES					
14. ABSTRACT Mutations in one allele TP53 gene in early stages frequently followed by the loss of the remaining wild-type allele (LOH) in later stages of tumor development. Despite the strong notion that p53LOH promotes tumorigenesis, its specific role in acute and long-term response to genotoxic modalities remained unclear. The major innovative findings for the reporting period are: 1) Using MMTV;ErbB2 mouse model carrying heterozygous R172H p53 mutation, we show that under normal condition, transcriptionally competent wtp53 allele enables the genomic integrity and suppresses the mTOR pathway in mutp53 heterozygous ErbB2 cancer cells; 2) In the long run, the single dose of irradiation of premalignant lesions accelerates mammary tumorigenesis, induces p53LOH and metastases that are more profound in the presence of mutant p53 allele; 3) As an early response in mutant p53 heterozygous cells, genotoxic stress promotes sustained mutant p53 stabilization, continuous DNA damage, and aberrant G1-S transition; 4) Mechanistically, the deficient cell cycle checkpoint coupled with inefficiently repaired DNA underlies the higher frequency of p53LOH in mutant p53 heterozygous cells; 5) The main physiological outcomes of p53LOH are profound stabilization of mutant p53 protein, mTOR upregulation, enhanced genomic instability, and metastases. Collectively, our results imply that in mutant p53 heterozygous cells, genotoxic stress facilitates the selective pressure for wtp53 loss. The latter enhances cancer cells fitness by mTOR upregulation and provides the genetic plasticity for the acquisition of metastatic properties.					
15. SUBJECT TERMS p53 loss of heterozygosity, mouse model of Her2 positive breast cancer, radiotherapy, genomic instability, mTOR pathway					
16. SECURITY CLASSIFICATION OF:			17. LIMITATION OF ABSTRACT	18. NUMBER OF PAGES	19a. NAME OF RESPONSIBLE PERSON
a. REPORT	b. ABSTRACT	c. THIS PAGE			19b. TELEPHONE NUMBER (include area code)
Unclassified	Unclassified	Unclassified	Unclassified	58	USAMRMC

Table of Contents

	<u>Page</u>
1. Introduction.....	1
2. Keywords.....	1
3. Accomplishments.....	1
4. Impact.....	16
5.Changes/Problems.....	17
6. Products.....	18
7. Participants & Other Collaborating Organizations.....	19
8. Special Reporting Requirements.....	21
9. Appendices.....	attached

1. INTRODUCTION:

Mutations in the p53 tumor suppressor gene are the most prevalent genetic events in human Her2-positive breast cancer and are associated with poor prognosis and survival. Frequently in the early stages of cancer, a p53 mutation in one allele is followed by loss of heterozygosity (LOH) in the second allele, during tumor progression. And despite a strong notion that p53 mutations with subsequent LOH are driving events in breast cancer, the translational significance of p53 mutational and LOH status, and their role in breast cancer development and progression have not been comprehensively evaluated, especially in the context of conventional genotoxic modalities. Previously we found that the heterozygous mutp53 R172H allele increases the frequency of p53 LOH in mammary tumors compared with the p53- null allele that correlates with aggravated tumorigenesis in an MMTV/ErbB2 mouse breast cancer model. This phenotype became even more prominent after γ -irradiation of mice with premalignant lesions, which led to a dramatic increase in metastases in the presence of mutp53 allele. These data strongly suggest that DNA damage further augments the oncogenic activity of mutp53. Thus, we hypothesize that at early stages of breast cancer, genotoxic therapies, in the long run, can promote tumor progression in mutp53 heterozygous tumors by (1) inducing the loss of the remaining wtp53 allele and thus, its tumor suppressor activity; (2) stabilizing mutp53 protein over the threshold needed to manifest its full oncogenic potential; (3) p53 LOH-mediated acquisition of metastatic properties; (4) amplifying ErbB2 and its related HSF1 (Heat Shock Factor1) signaling. This study aims to evaluate the physiological consequences of p53 LOH in breast cancer initiation, progression, and metastases and assess how mutp53 affects response to genotoxic therapies with regard to p53 LOH status; how the response changes at different stages of breast cancer; and the short- and long-term therapeutic effects of genotoxic treatments.

The major accomplishments of the project up-to-date

2. KEYWORDS: p53, mutant p53, ErbB2, Her2, breast cancer, loss of heterozygosity (LOH), radiation, chemotherapy, Her2 positive breast cancer.

3. ACCOMPLISHMENTS:

The major goals of the project are:

Major Task 1. Determine the effect of DNA-damaging therapeutics on p53 LOH and tumorigenesis in ErbB2- driven mutp53 mammary tumors in vivo.

Subtask 1. Define the physiological consequences of p53 LOH in ErbB2-driven mammary tumorigenesis. *Analyze histopathology, the ErbB2/HSF1 signaling by IHC and Western in the established collection of mammary tumors from irradiated and non-irradiated mice with different p53 LOH status. (timeline months: 1-12, 100% completion).*

We have previously shown that mutp53 amplifies ErbB2 signaling via stimulation of Heat Shock Transcription Factor 1 (HSF1) and its transcriptional target Heat Shock Protein 90 (Hsp90), which, in turn, stabilizes numerous Hsp90 clients, such as ErbB2 and mutp53 itself^{1,2}. Therefore, we examined how p53LOH affects mutp53-HSF1-ErbB2 feed-forward loop in mammary tumors of mice with different p53 genotypes and experimental conditions.

First, we assessed mutp53 protein level through systematic IHC analysis of mammary tumors from irradiated and non-irradiated mice.

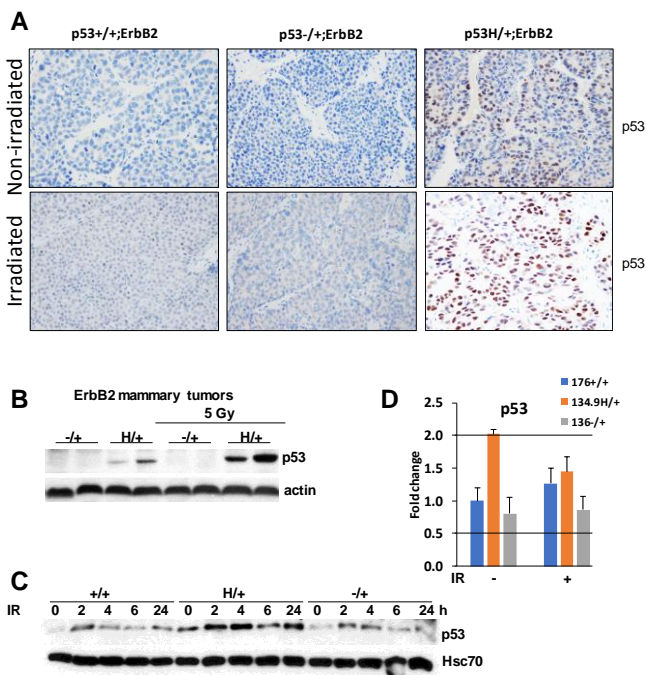


Fig. 1. Irradiation induces the accumulation of mutant p53 protein in heterozygous cancer cells.

(A) The increase in p53LOH in H/+;ErbB2 mammary tumors are associated with the stabilization of mutp53 after irradiation of premalignant lesions, while irradiation did not affect wtp53 levels in +/+;ErbB2 and -/-;ErbB2 tumors. Representative images of p53 IHC of mammary tumors with indicated genotypes that were non-irradiated (upper panels) and irradiated (lower panels). 4 tumors per genotype were analyzed. **(B)** irradiation stabilizes mutp53 protein in mutp53 heterozygous tumors, but not in -/+;ErbB2 tumors. Western blot 16h after irradiation *in vivo*. **(C)** wtp53 in +/+;ErbB2 cells was only transiently upregulated at 2h post-irradiation (9Gy), mutp53 shows much higher and continuous stabilization in H/+;ErbB2 cells. **(D)** No increase in p53 RNA was found in H/+;ErbB2 cells after irradiation *in vitro*. QRT-PCR.

The majority of homozygous mutp53 human cancers and cell lines are known to accumulate high levels of mutp53 protein mainly due to its failure to transactivate E3 ligase Mdm2. However, little is known about how mutp53 protein levels are regulated in heterozygosity. Consistent with our previous study on R248Q;MMTV-Neu mouse model³, we found only 10-15% of p53 positive cells in H/+;ErbB2 mammary tumors, while no p53 staining was detected in p53-/-;ErbB2 and +/+;ErbB2 tumors (Fig. 1A, upper panel). The increase in p53LOH in H/+;ErbB2 mammary tumors was associated stabilization of mutp53 after irradiation of premalignant lesions (Fig. 1A, lower panel). Conversely, irradiation did not affect wtp53 levels in +/+;ErbB2 and -/-;ErbB2 tumors (Fig. 1A, lower panel). As mutp53 stabilization in tumors was proposed to be essential for its oncogenic function⁴, p53LOH with subsequent mutp53 stabilization may represent a key event in cancer progression *in vivo*.

To understand how irradiation affects mutp53 protein levels in heterozygosity, H/+;ErbB2 and -/+;ErbB2 mice were irradiated or not at the time of tumor onset (tumor volume-1cm³). Western blot of tumors 16h after irradiation revealed that irradiation stabilizes mutp53 protein in heterozygous tumors significantly higher than wtp53, as p53 in -/+;ErbB2 tumors remained undetectable (Fig. 1B). Likewise, murine mammary tumor cell

lines show different kinetic of wtp53 and mutp53 stabilization following irradiation (9Gy). While wtp53 in +/+;ErbB2 cells was only transiently upregulated at 2h post-irradiation, mutp53 shows much higher and continuous stabilization in H/+;ErbB2 cells (Fig. 1C).

As the previous study has shown upregulation of mutp53 RNA in response to genotoxic anthracyclines in human cell lines⁵, we analyzed p53 mRNA in cells with different genotypes before and after irradiation. We found no increase in p53 RNA in H/+;ErbB2 cells (Fig. 1D), suggesting post-transcriptional regulation of mutp53 protein levels in heterozygosity in response to irradiation. It still remains to be elucidated how mutp53 protein level is regulated in heterozygosity in response to DNA damage.

Collectively our data led us to hypothesized that in heterozygous cells, irradiation stabilizes mutp53 over the threshold, which is sufficient to promote its oncogenic activities leading to p53LOH and tumor progression.

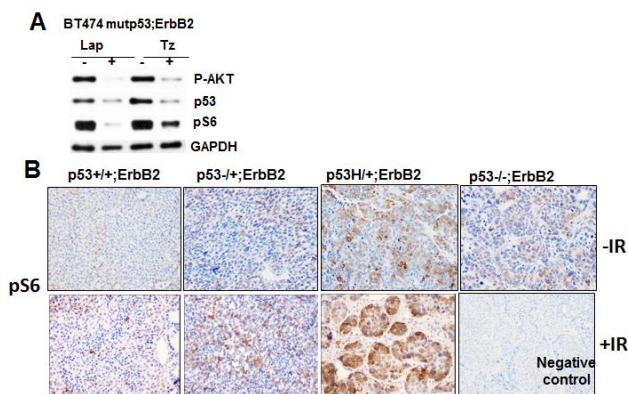


Fig. 2. P53LOH is associated with the activation of the mTOR pathway. (A) ErbB2 inhibition by lapatinib and trastuzumab inhibits mTOR(pS6) in human mutp53 BT474 cells (B) Irradiation-induced p53LOH is concomitant with upregulation of mTOR signaling (lower panel) that is more profound in mutp53 heterozygous tumors. 4 tumors per genotype were analyzed. Representative images.

Next, we asked how irradiation-induced p53LOH affects ErbB2 signaling by systematic analysis of ErbB2 IHC staining of mammary tumors with a different p53 genotype that were irradiated or not. However, the strong immunostaining of all mammary tumors independently of genotype precluded the quantitative and conclusive evaluation. As an alternative approach, we analyzed the mTOR (mammalian target of rapamycin) pathway, as a key downstream target of ErbB2 signaling. mTOR pathway plays an essential role in regulating many oncogenic processes - protein synthesis, metabolism, autophagy, and, most importantly, genomic instability

in different cancer types⁶⁻⁸, including breast cancer^{6,9}. Indeed, specific inhibitors of ErbB2 lapatinib and trastuzumab effectively suppress mTOR in human mutp53;ErbB2 (BT474) cells, as indicated by downregulation of pS6, a downstream target of mTOR (Fig. 2A). We found that irradiation exacerbates p53LOH that is concomitant with upregulation of mTOR signaling predominantly in mutp53 heterozygous tumors (Fig. 2B). Therefore, p53LOH followed by upregulation of the mTOR pathway can cause the major shift to more malignant phenotype by activating of the whole array of oncogenic events mediated by mTOR. In **Major Task 2, Subtask 3** we explored the mechanistic link between p53LOH and the mTOR pathway.

Previously we and others^{10,11} have shown that ErbB2 signals via the phosphoinositide-3-kinase (PI3K)-AKT-mTOR axis to phosphorylate HSF1 at pSer326 leading to transcriptional activation of HSF1. On the other hand, the specific inhibitor of mTOR, rapamycin, inhibits HSF1¹⁰. Therefore, we hypothesized that p53LOH via stimulation of the mTOR pathway leads to HSF1 activation. To test this hypothesis, we stained

mammary tumors from irradiated/non-irradiated mice with different genotypes with HSF1 antibody. However, all HSF1 antibodies, which showed highly specific IHC staining in human specimens¹, produced a substantial background staining in mouse tissues. As an alternative to IHC study, we utilized *in vitro* approach to investigate how p53LOH affects HSF1 activity (**Major Task 2, Subtask 3**).

Subtask 2. Evaluate the effect of different p53 mutations on p53 LOH in ErbB2-driven mammary tumorigenesis.

Test whether similar to R172H, R248Q mutant p53 allele aggravates mammary tumorigenesis compared to p53 null counterparts and promotes p53 LOH after irradiation. (timeline months: 1-24, 50% completion)

In the previous progress report, we demonstrated that in contrast to R172H p53 mutation, breast cancer latency and the survival between p53R248Q/+;Neu and p53-/+;Neu siblings were similar. These results implicate p53 mutation-specific effects on mammary cancer development and progression in ErbB2 context. Although further experimental proofs are needed, this data highly suggests that physiological outcomes of irradiation in p53R248Q/+;Neu mice would be similar to -/+;ErbB2 mice, which we extensively evaluated in the current study. If so, the potential impact of these experiments is not expected to be high. Therefore, instead of perusing of this subtask, we dedicated the time and resources to investigate the mechanism, by which mutp53 promotes p53LOH (**Major Task 2, Subtask 3**). Although beyond the originally proposed study, this knowledge may have a significant clinical impact, as it will help to understand how mutp53 heterozygous tumors in early stages respond to DNA damage and to identify the potential targets to prevent the adverse effects of genotoxic therapies in early stages of breast cancer. Since irradiation and the evaluation of p53R248Q/+;Neu mouse model are technically straightforward, we will continue this study after completion of more impactful subtasks.

Subtask 3. Assess the effect of irradiation of established mutp53;ErbB2 tumors on p53 LOH (neoadjuvant setting). Test whether irradiation of established tumors induces LOH and accelerates mammary tumorigenesis in R172H/+;ErbB2 mice.

First, we will expand our breeders colonies to generate 60 females of each genotypes: p53-/+;ErbB2, H/+;ErbB2 and +/+;ErbB2. (timeline: months 1-12, 80% completion). 30 mice of each genotypes will be irradiated with a single dose of 5Gy irradiation at the time of tumor presentation. The monitoring and analysis as described for the Aim1b. 60 females p53-/+;ErbB2 + 60 females H/+;ErbB2 60 females +/+;ErbB2 = 180 total animals. (timeline: months 12-32, 30% completion).

Of the generated mice, 7 of p53-/+;ErbB2, 7 of p53H/+;ErbB2 and 1 of p53+/+;ErbB2 had developed tumors and were then subjected to a single dose of irradiation at the time of tumor presentation. Tumor growth per mouse was then followed and analyzed as described in Aim1b. Although this experiment is still ongoing, among the analyzed mice subjected to irradiation we observed the genotype-specific differences. First, similar to irradiation of pre-malignant lesions, we observed that the presence of mutp53 allele facilitates p53LOH in

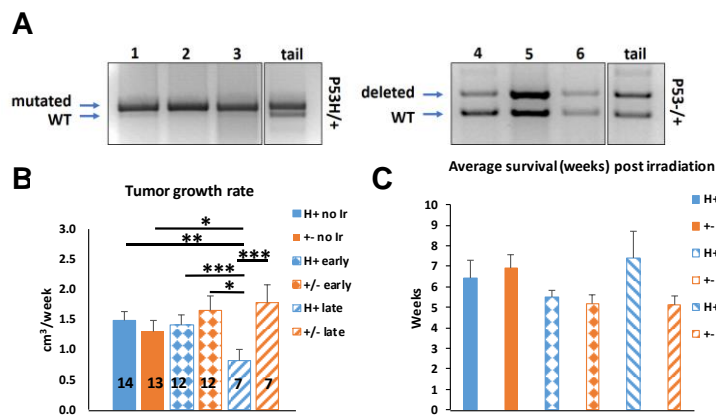


Fig. 3. P53LOH in tumors irradiated in the neoadjuvant setting. (A) LOH was observed in p53H/+;ErbB2 (lanes 1-3), but not in p53-/+;ErbB2 tumors (lanes 4-6). Each lane represents one tumor from one mouse. (B) Tumor growth rate after irradiation in the neoadjuvant setting. The reduction in tumor growth rate of p53H/+;ErbB2 tumors, but not p53-/+;ErbB2 tumors, when irradiated at tumor onset (late), as compared to p53-/+;ErbB2 and p53H/+;ErbB2 tumors when irradiated premalignant (early). *= $p \leq 0.05$; ***= $p \leq 0.001$, **= $p \leq 0.01$. (C) Survival analysis of mice irradiated at the time of tumor onset. The difference did not reach significance due to a low number of mice per group. Survival was measured from the day the tumor was 1cm³ to end-point (largest tumor 4cm³ or adverse side effects). SE bars are shown.

established mammary tumors as compared to p53-/+;ErbB2 (Fig. 3A). Second, as a short response, irradiation leads to a reduction in tumor growth in the presence of mutp53 allele compared to -/+;ErbB2 tumors (Fig. 3B). This seeming contradiction with the data on irradiation of pre-malignant lesions (see preliminary data for grant application) can be explained by our *in vitro* results (Fig. 6). We found that after irradiation, in contrast to a deep G1 arrest in p53-/+;ErbB2 cells, H/+;ErbB2 cells are able to evade the checkpoint and go through G1-S transition without proper DNA repair. In the short term, this abnormal cell cycling may lead to mitotic catastrophe in cells, which have received extensive DNA damage. However, in the long term, surviving mutp53 cells may accumulate abundant genomic aberrations (p53LOH as an example) leading to metastases and chemoresistance. At this point, due to a low number of analyzed mice, we cannot conclusively demonstrate whether irradiation in the neoadjuvant setting affects the survival of mice in the genotype-specific manner (Fig. 3C). In the next funding period we will continue implication of this subtask to achieve statistically significant results and to validate our mechanistic study *in vitro* (Major Task 2, Subtask 3).

Subtask 4. Determine whether generic genotoxic drug doxorubicin promotes p53 LOH in established R172H/+;ErbB2 tumors in the neoadjuvant setting.

To test whether commonly used for Her2 positive breast cancer treatment genotoxic drug doxorubicin similar to irradiation induces LOH in mutp53 dependent manner, 30 H/+;ErbB2 females, 30 p53-/+;ErbB2 and 30 +/+;ErbB2 females will be treated with 4mg/kg doxorubicin (dox) in PBS intraperitoneally at the time of tumor onset (0.5 cm³, volume) once daily for 5 consecutive days. Monitoring and analysis will be performed as described in Aim 1b.

60 females p53-/+;ErbB2 + 60 females H/+;ErbB2 + 60 females +/+;ErbB2 = 180 total animals (timeline: months 12-32, 30% completion).

For the implementation of this subtask, we expanded the colonies of mice with different p53 genotypes. At the present moment, we are expecting the emergence of tumors to start the treatment protocol and the evaluation of tumor growth kinetics in the context of p53LOH.

Major Task 2. Mechanistically assess the physiological consequences of p53 LOH in heterozygous mutp53 mammary cells in vitro.

Subtask 1. Examine the frequency and time of p53 LOH onset in existing collection of cell culture of primary mammary epithelial cells and mammary tumors culture derived from mice with different p53 genotypes. Serial passaging of R172H/+;ErbB2 vs p53-/+;ErbB2 vs p53+/+;ErbB2 MECs and mammary tumors cultured cells. (timeline: months 12-24, 100% completion).

We previously reported that our attempts to continuously passage MECs from H/+;ErbB2, -/+;ErbB2 and +/+;ErbB2 mice were not successful. This is in contrast to H/H;ErbB2 and -/-;ErbB2 MECs. All wtp53 expressing MECs underwent senescence following passage 3. This data is consistent with our observations that wtp53 in heterozygosity is competent to exert its tumor suppressive function by inducing the transcription of a subset of target genes (Fig. 5 A,D,E). Therefore, we have focused on studying *in vitro* cell lines, which we established from mammary tumors of mice with different p53 genotype. Contrary to MECs, mammary tumor cell lines independently of p53 genotype can be continuously passaged.

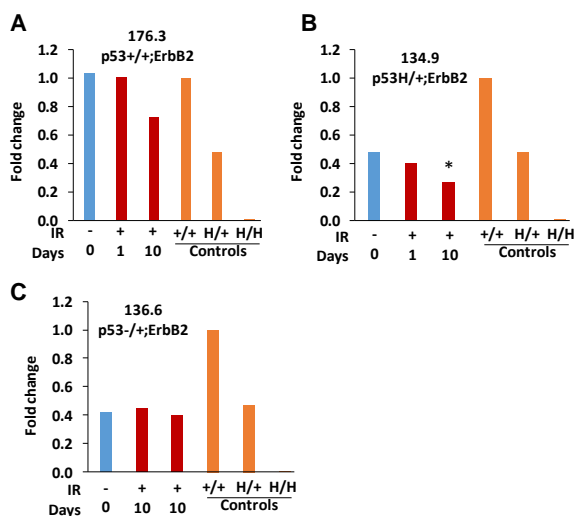


Fig. 4. Mutp53 enhances LOH following γ -irradiation in cell culture.

Cultivated mammary tumors cells were irradiated (9Gy), or not, and grown up to 10 days post-irradiation. DNA was extracted at the indicated time points. The copy number of p53 wt and mut alleles was quantified by real-time PCR. DNA extracted from tail tissue samples of the corresponding genotype was used for copy number control. The experiment was repeated three times. Summary of a representative experiment.

Since the standard PCR cannot quantitatively evaluate the change in copy number of either allele, we utilized quantitative PCR (qPCR) with primers that are specific for either mutp53 or wtp53 alleles. The primers were designed to detect the nucleotide point mutation G-A that results in amino acid mutation R172H. The specificity of the primers was validated by DNA extracted from +/+;ErbB2, H/+;ErbB2, -

/+;ErbB2, -/-;ErbB2 and H/H;ErbB2 mouse tails. No cross-reactivity between mutp53 and wtp53 allele and *vice versa* was detected. Genotypes of generated cell lines were confirmed by real-time PCR (Fig. 4, blue bar). Surprisingly, all established tumor cell lines continuously maintained heterozygosity during passaging in culture (Fig. 4, blue bar). Although we expected that passaging would cause the gradual loss of wtp53 allele in heterozygous cells, the stable maintenance of heterozygosity under normal condition makes our study of irradiation-induced p53LOH *in vitro* straightforward.

Subtask 2. Test the effect of irradiation on the frequency and time of p53 LOH onset in primary mammary epithelial cells (MECs) and mammary tumors culture derived from mice with different p53 genotypes. Serial passaging of R172H/+;ErbB2 vs p53-/+;ErbB2 vs p53+/+;ErbB2 MECs and mammary

tumors cultured cells after single dose of irradiation *in vitro* at passage 1. (timeline: months 24-32, 100% completion).

To validate our *in vivo* data, cell lines with different genotype were irradiated, or not, with a single dose of 9Gy and the copy number of wtp53 and mutant (R172H) alleles were determined by real-time PCR at different time points as indicated in Fig. 4. In agreement with *in vivo* data, we found the profound loss of wtp53 allele after irradiation in p53H/+;ErbB2, but not in p53-/+;ErbB2 cell lines 10 days after irradiation (Fig. 4B,C). Irradiation-induced a marginal decrease in copy number of wt allele in 176.3+/+;ErbB2 cell line (Fig. 4A). This data is in complete agreement with our results *in vivo*. Therefore, we successfully established *in vitro* model for studying the effects of p53LOH well-controlled setting. We will utilize this model to determine the mechanism, by which mutp53 allele in heterozygosity promotes p53LOH and tumor progression (**Major Task 2, Subtask 3**).

Collectively, our *in vivo* and *in vitro* data indicate that mutp53 allele in heterozygosity enhances p53LOH after irradiation.

Subtask 3. Correlate the p53 LOH status of R172H/+;ErbB2 vs. p53-/+;ErbB2 vs. p53+/+;ErbB2 MECs and mammary tumors cultured cells with cellular properties (proliferation, chemoresistance, allografts) and with biochemical characteristics (ErbB2 and HSF1 signaling). (timeline: months 24-32, 60% completion).

As a part of the completion of this subtask, we performed a series of mechanistic studies that were not originally planned in the grant application. These experiments were done to strengthen our study and to identify the mechanism by which mutp53 stimulates p53LOH in response to irradiation.

To evaluate *in vitro* the consequences of p53LOH with respect to the transcriptional activity of wtp53 in heterozygosity we studied the expression of canonical p53 target genes Mdm2 and p21 in response to Mdm2 inhibitor nutlin by QRT-PCR. Contrary to genotoxic treatments (irradiation, chemotherapeutics), nutlin was shown to promote p53 transcriptional activity without induction of DNA damage or other off-target effects. No significant difference in the expression of Mdm2 and p21 was observed between p53+/+;ErbB2 and H/+;ErbB2 cells, while nutlin failed to induce p53 targets in H/H;ErbB2 and -/-;ErbB2 MECs (Fig. 5A). Hence, in heterozygosity mutp53 cannot fully exert its tumorigenic dominant-negative function, whereas p53LOH leads not only to loss wtp53 tumor-suppressive activities, but also empowers mutp53 gain-of-function.

P53LOH is associated with the activation of the mTOR pathway.

Our *in vivo* analysis demonstrated that irradiation-induced p53LOH in mutp53 heterozygous tumors was associated with substantial upregulation of the mTOR pathway (Fig. 2B). Since the mTOR pathway is a key downstream target of ErbB2 signaling, we evaluated *in vitro* how mTOR pathway is regulated in heterozygosity and how p53LOH affects ErbB2-mTOR-HSF1 axis. Several studies have shown that wtp53 inhibits the mTOR pathway via induction the expression of Sestrin 1 and 2, that interact and activate AMPK leading to mTOR inhibition^{12,13}. In agreement with these findings, we found the elevated mTOR signaling in mutp53;ErbB2 vs.

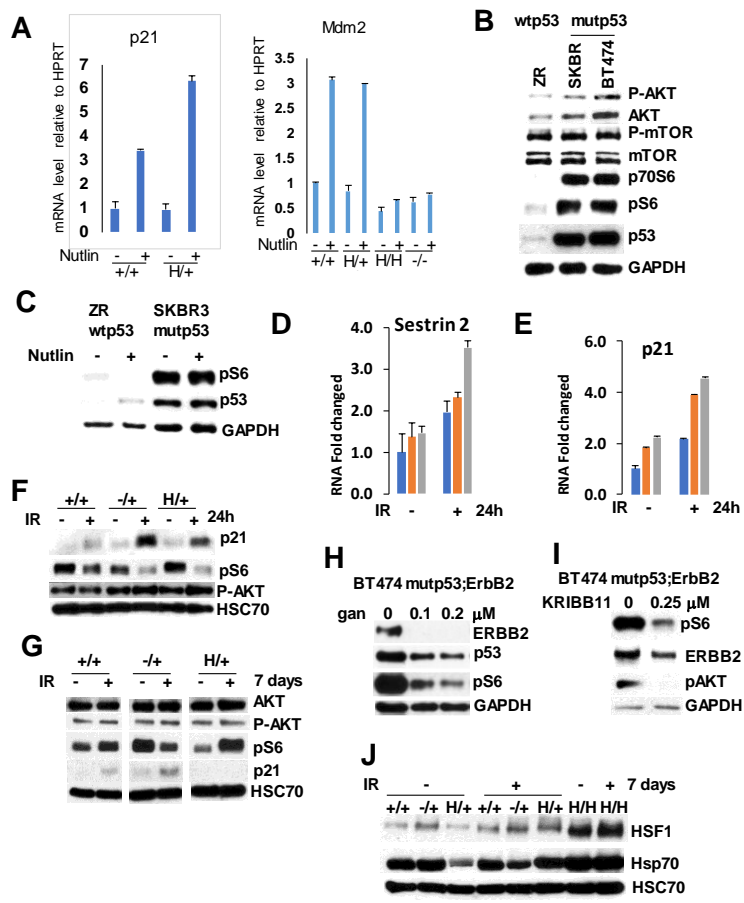


Fig. 5. P53LOH is associated with the activation of the mTOR pathway. (A) In mutp53 heterozygous cells, wtp53 retains its transcriptional activity and induces its target p21 and Mdm2 in response to Mdm2 inhibitor nutlin. Nutlin does not induce Mdm2 in H/H;ErbB2 and -/-;ErbB2 MECs (right, bars 5-8). (B) mTOR (pS6) is more activated in mutp53;ErbB2(BT474, SKBR3) than in wtp53 cells (ZR75-30). (C) Upregulation of wtp53 by nutlin suppresses mTOR signaling in wtp53;ErbB2 cells ZR 75-30, but not in mutp53;ErbB2 SKBR3 cells. (D) Irradiation induces RNA expression of p53 targets Sestrin 2 (D) and p21 (E) in all genotypes +/+;ErbB2(blue), H/+;ErbB2 (red) and -/+;ErbB2(gray) cells. QRT-PCR 24h post-irradiation. (F) irradiation in the short term (24h) leads to downregulation of mTOR activity in the presence of wtp53 allele. (G) irradiation-induced p53LOH in H/+;ErbB2 cells is associated with upregulation of mTOR and lack of detectable p21. This is in contrast to +/+;ErbB2 and -/+;ErbB2 cells. Western blot 7 days post-irradiation. Hsp90 inhibition by ganetespib (H) and HSF1 inhibition by KRIBB11 (I) suppresses mTOR in mutp53 human BT474 cells. Western blot after 24h treatment with indicated concentrations. (J) p53LOH after irradiation is associated with both mTOR and HSF1 activation (as indicated by elevated Hsp70) only in H/+;ErbB2 cells. Western blot 7days after irradiation.

wtp53;ErbB2 human cancer cells as indicated by high levels of downstream effectors of mTOR - p70S6 and pS6, whereas the level of mTOR and p-mTOR protein were comparable (Fig. 5B). Furthermore, upregulation of wtp53 by nutlin suppresses mTOR signaling in wtp53;ErbB2 cells ZR 75-30, but not in mutp53;ErbB2 SKBR3 cells (Fig. 5C). Consistent with transcriptional activity of wtp53 in heterozygosity (Fig. 5A), Sestrin 2 and p21 RNA expression was upregulated 24h post-irradiation in all genotypes +/+;ErbB2, -/+;ErbB2 and H/+;ErbB2 cells (Fig. 5D,E) that was associated with downregulation of mTOR activity (Fig. 5F). Importantly, irradiation did not alter pAKT, the upstream effector of mTOR (Fig. 5F) indicating that the modulation of Sestrins by wtp53 is the main regulator of mTOR activity after irradiation.

To establish how p53LOH affects mTOR activity we tested cells 7 days after irradiation the time point when ~50% of H/+;ErbB2 cells underwent p53LOH (Fig. 4B). Remarkably, we found that the loss of wtp53 allele in H/+;ErbB2 cells was associated with profound upregulation of mTOR and lack of detectable p21 (Fig. 5G). No such effect was observed in +/+;ErbB2. Consistent with the retention of wtp53 allele, irradiation leads to sustained

mTOR inhibition in -/+;ErbB2 cells, which was concomitant with chronic p21 upregulation (Fig. 5G). Similar effects of irradiation we observed *in vivo*. Irradiation exacerbates p53LOH that is concomitant with upregulation of mTOR signaling predominantly in mutp53 heterozygous tumors (Fig. 2B).

Next, we asked whether mutp53 itself has a functional impact on the mTOR pathway. We have previously shown that mutp53 amplifies ErbB2 signaling via stimulation of Heat Shock Transcription Factor 1 (HSF1) and its transcriptional target Heat Shock Protein 90 (Hsp90), which, in turn, stabilizes numerous Hsp90 clients, such as ErbB2 and mutp53 itself^{1,2,10}. On the other hand, as Hsp90 clients, the components of the mTOR pathway, (<https://www.picard.ch/downloads/Hsp90interactors.pdf>), may also be stabilized by mutp53-HSF1-Hsp90 loop. In agreement, both Hsp90 inhibitor, ganetespib, (Fig. 5H) and HSF1 inhibitor, KRIBB11, (Fig. 5I) efficiently suppress mTOR signaling. Furthermore, p53LOH after irradiation was associated with both mTOR and HSF1 activation (as indicated by elevated Hsp70) only in H/+;ErbB2 cells (Fig. 5J). Hence, in addition to the loss of wtp53 suppressive activity, p53LOH may lead to mTOR activation via stimulation HSF1-ErbB2 axis in mutp53 dependent manner, providing the survival advantage over to p53+/+;ErbB2 and p53-/+;ErbB2 cells. Therefore, the activation of the mTOR pathway associated with p53 LOH generates the selective pressure for the loss of wtp53 allele specifically in mutp53 heterozygous cells.

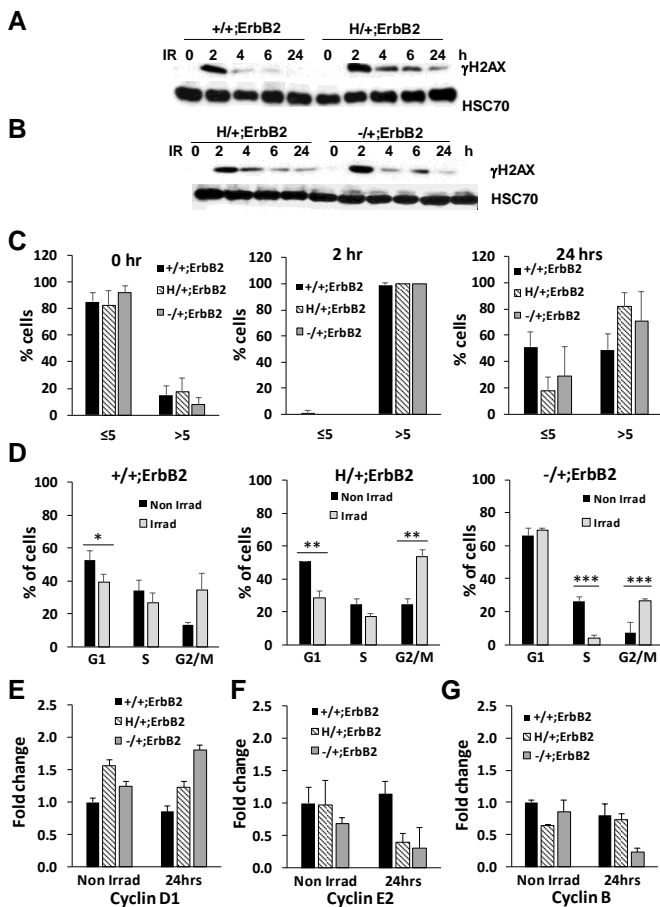


Fig. 6. (A) The single dose of γ -irradiation (9Gy) induces sustained DNA damage up to 24h in H/+;ErbB2 and -/+;ErbB2 cells (B), but is efficiently resolved in +/+;ErbB2 cells. γ H2ax Western blot (A). (C) Quantification of cells with >5 and <5 γ H2AX foci/cell in 10 random fields in p53+/+, p53H/+ and p53 -/+ cell lines, before and after γ -irradiation (9Gy, 2 and 24h post-irradiation). (D) Aberrant cell cycle check point following γ -irradiation in H/+;ErbB2 cells. Bar graphs showing cell cycle analysis of p53+/+;ErbB2 p53H/+;ErbB2, and p53 -/+;ErbB2 cell lines irradiated (gray bars) or not (black bars). Impact of the single dose of γ -irradiation (9Gy) on the transcription of Cyclin D1 (E), Cyclin E2 (F), Cyclin B (G). QRT-PCR 24h post-irradiation.

Aiming to identify the mechanism, by which mutp53 promotes p53 LOH, we analyzed the kinetics of DNA damage and cell cycle profiles after irradiation. It is generally accepted that wtp53 upon genotoxic stress activates the transcription of genes involved in cell-cycle arrest and DNA repair or apoptosis, protecting the genome integrity. Contrary, mutp53 proteins may perturb these genome-guarding mechanisms and promote various types of genomic instability¹⁴. Yet, how p53 heterozygous cells respond to DNA damage is not fully understood. Hence, we irradiated (9 Gy) p53+/+;ErbB2, p53-/+;ErbB2 and p53H/+;ErbB2 cells *in vitro* and examined the extent of DNA damage using γ H2AX as a marker of DNA double-strand breaks (DSBs). Both, γ H2ax Western blot analysis (Fig. 6A, B) and count cells with γ H2ax foci (Fig. 6C) have shown sustained DNA damage up to 24h in heterozygous cells (Fig. 6A-C). Conversely, in +/+;ErbB2 cells, γ H2AX peak at 2hr post-irradiation was

efficiently resolved by 4hr and resumed to a normal level by 24hr post-irradiation (Fig. 6A,C). These results suggest that, while p53+/+ cells exhibit a functional DNA damage response, cells heterozygous or hemizygous for wtp53 manifest persistent DNA damage due to a deficient DNA repair following γ -irradiation.

To further investigate the mechanism by which mutp53 may cause genomic abnormalities we compared cell cycle profiles of cells with various genotypes at 24hr following γ -irradiation. Both p53+/+;ErbB2 and p53 -/+;ErbB2 cells exhibited comparable cell cycle profiles before irradiation (50% G1, 35% S, 15% G2/M and 65% G1, 30% S, 5% G2/M, respectively), whereas p53H/+;ErbB2 cells showed an abnormal cell cycle distribution with lower G1 (~40%) and S (~20%) and significantly higher G2/M (~40%) indicating an increased rate of proliferation (Fig. 6D). Consistent with fast recovery from DNA damage after irradiation, p53+/+;ErbB2 cells did not significantly change G1 and S content and a slight increase in G2/M arrest (Fig. 6D). Importantly, persistent DNA damage induced by irradiation leads to G1, G2/M arrest and significantly reduced S (2%) in -/+;ErbB2 cells (Fig. 6D) indicating the complete block of G1-S transition. Contrary, H/+;ErbB2 cells continue to go through cell cycle even in the presence of damaged DNA (Fig. 6A,B) as indicated by unchanged S phase and an increase in G2/M (~60%) (Fig. 6D). Therefore, in mutp53 heterozygous cells, aberrant G1-S transition coupled with inefficiently repaired DNA generates the genomic perturbations that facilitate p53LOH. Followed by p53LOH, the upregulation of the mTOR pathway further enhances the fitness of cancer cells enabling cell survival after DNA damage.

Next, to determine how the cell cycle is regulated in cells with different p53 genotypes, we evaluated the expression of cyclin D1, cyclin E, and cyclin B 24h after irradiation. Cyclin D1 is a labile nuclear protein that is essential for G1-S progression¹⁵⁻¹⁷. Cyclin D1 level varies depending on the cell cycle phase; high during G1 and G2/M and low during S¹⁵⁻¹⁷. We found no significant difference in cyclin D1 transcription at the basal level in all three genotypes (Fig. 6E), though p53H/+ cell line tended to have higher level reflecting a higher overall proliferation. Consistent with unchanged after irradiation S phase, cyclin D1 transcription level remained unaffected in both p53+/+;ErbB2 and p53H/+;ErbB2 cell lines as compared to the non-irradiated controls (Fig.6E). In agreement with G1 arrest after irradiation, p53-/+;ErbB2 cells showed the highest increase in cyclin D1 transcription (Fig. 6D).

Next, we examined the transcription levels of cyclin E2. Cyclin E2 was shown to prepare cells for DNA replication during the G1-S transition and is required for centrosome duplication in the S phase¹⁸. While there was no significant difference in cyclin E2 transcription level in all three non-irradiated cell lines, both p53H/+;ErbB2 and p53-/+;ErbB2 cells showed a significant reduction in cyclin E2 transcription (Fig. 6F). This result suggests, that DNA damage induces growth arrest in -/+;ErbB2 cells, while this mechanism malfunctions in mutp53 heterozygous cells, which enter into S phase unprepared for both correct centrosome and DNA duplication.

Cyclin B is required for mitotic spindle assembly and entry into mitosis¹⁹. As shown in Fig. 6G, there was no significant difference in cyclin B transcription level prior to irradiation in all three cell lines. However, radiation induces a significant reduction in cyclin B transcription only in p53-/+ cell lines, indicating a block in

entering mitosis. In agreement with elevated after irradiation G2/M phase, cyclin B shows a marginal increase in H/+;ErbB2 cells suggesting the transition to mitosis with unrepaired DNA.

Collectively our results suggest that after genotoxic stress, stabilized mutp53 in heterozygosity (Fig. 1C) overrides wtp53 genome-guarding function leading to the deficient cell cycle checkpoint (high p21 and low cyclin E2) and drives the cell through S phase to enter mitosis (high G2/M) before DNA is repaired (high γ H2AX), and with impaired mechanism of centrosome duplication (low cyclin E2). Together, these cell cycle malfunctions may lead to accumulation of chromosomal aberrations and p53LOH in mutp53 heterozygous cells.

p53LOH is associated with the switch from HRR to NHEJ and genomic instability.

Our results suggest that the key mechanism, by which mutp53 induces p53LOH in response to DNA damage, is the deficient DNA repair coupled with deficient checkpoint and aberrant cell cycle progression. Hence, we focused on basic DNA repair mechanisms that can underlie p53 genotype-specific response to irradiation that can lead to p53LOH in the presence of mutp53.

Genomic instability, such as chromosomal rearrangement, has been attributed as one of the major causes of LOH^{7,14}. Chromosomal rearrangements are caused mainly by failures in normal chromosome segregation during the mitotic process. Mutations in a number of genes (p53, PI3K, KRAS, TGF β) were shown to hinder normal mitosis leading to chromosomal aberrations²⁰. Also, the accumulation of various mutations during cancer progression can be a result of the failure of proper DNA repair.

Wtp53 is activated in response to a range of stress signals, and it suppresses cellular transformation by triggering a cell-cycle arrest, DNA repair, and apoptosis^{14,21}. Depending on cell context and the extent of DNA damage, p53 may elicit DNA repair by either, or both, of the two major repair pathways: 1) homologous recombinational repair (HRR)^{22,23}, and 2) nonhomologous end joining (NHEJ)²³⁻²⁵. HRR is relatively slow and less error-prone, while NHEJ is more error-prone²⁶.

We found that HRR (Rad51 as a marker) is active in +/+;ErbB2, H/+;ErbB2 and p53-/-;ErbB2 but, is suppressed in H/-;ErbB2 and H/H;ErbB2 mammary tumors (Fig. 7A). On the other hand, we found that wtp53 inhibits NHEJ (Ku70 as a marker) in ErbB2-driven mammary tumors, as we observed higher Ku70 staining in cells lacking wtp53 (Fig. 7B). Hence, in the context of p53 heterozygosity, the presence of wtp53 allele shifts the DNA repair mechanism towards to HRR, whereas p53LOH switches to low fidelity NHEJ DNA repair. Therefore, we hypothesized, that p53-genotype dependent switch from high fidelity to error-prone DNA repair mechanism leads to the acquisition of multiple mutations, which, in turn, induce mitotic abnormalities and chromosomal aberrations.

Chromosomal aberrations can be measured by the frequency of 'anaphase bridges' (AB) in the anaphase of the cell cycle. AB is defined as extended chromosome bridging between two spindle poles (Fig. 7C) and is a histologic hallmark of dicentric chromosomes²⁷. High AB was shown to be associated with the increased frequency of Apc LOH in Apc +/- Cdx2 +/- colon cancer mouse model⁷. Hence, we scored AB in

ErbB2 mammary tumors with different p53 genotypes. We found a marginal difference in AB between p53^{+/+};ErbB2, p53^{-/-};ErbB2, and p53^{H/+};ErbB2 mammary tumors, whereas genetic lack of wtp53 allele in context of heterozygosity markedly increased AB in mammary tumors of ErbB2 mice (Fig 7C). Next, to test an impact of mutp53 on AB formation, we analyzed another ErbB2 mouse model with conditionally-inactivatable upon tamoxifen administration R248Q mutp53 (floxR248Q^{-/-};ErbB2, flQ^{-/-};ErbB2 thereafter). First, we found elevated AB independently of the type of p53 mutation (R172H and R248Q) compared to p53^{-/-} tumors (Fig 7D). Second, genetic ablation of R248Qp53 *in vivo* significantly reduced the mutp53 protein level in established ErbB2 tumors, compared to vehicle-treated tumors (Fig 7E) and was concomitant with a two-fold AB decrease (Fig 7D). In

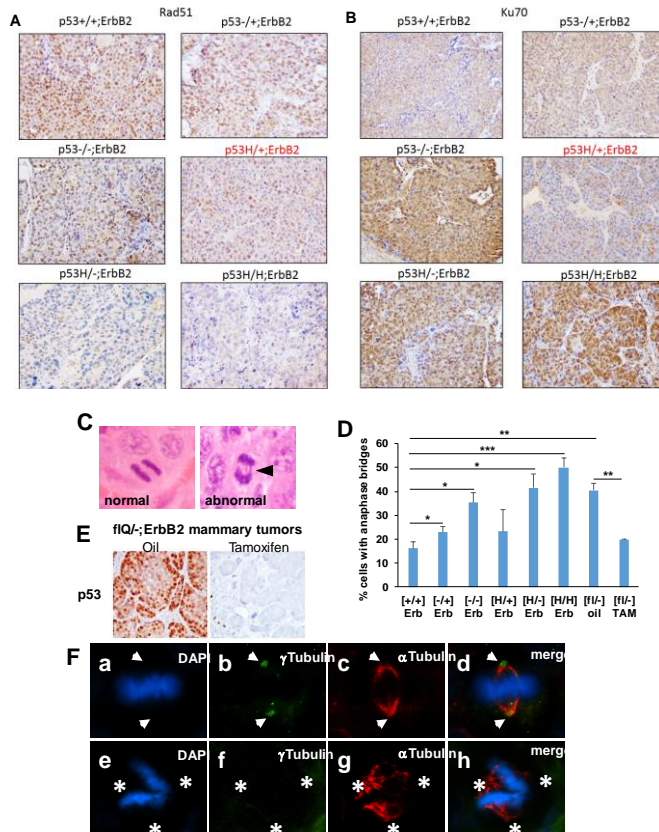


Fig. 7. p53LOH is associated with the switch from homologous recombinational repair (HRR) to nonhomologous end joining (NHEJ) and genomic instability. (A) Rad51 (marker for HRR) IHC in ErbB2 mammary tumors of mice with indicated p53 genotypes. **(B)** Ku70 (a marker for NHEJ) in ErbB2 mammary tumors of mice with indicated p53 genotypes. Four mammary tumors per genotype were stained. Representative images. **(C)** H&E staining of normal anaphase showing the segregating masses of chromosomes and bridging (arrow) between the segregating masses of chromosomes during anaphase. **(D)** Quantification of anaphase bridges (AB) in ErbB2 mammary tumors of mice with indicated p53 genotypes. *= $p \leq 0.05$; ***= $p \leq 0.001$, **= $p < 0.01$. **(E)** IHC of p53. Left panel: staining in the tumor from flR248Q^{-/-};ErbB2 mouse injected with oil, right panel: the depletion of p53 in the tumor from flQ^{-/-};ErbB2 mouse following tamoxifen injection. **(F)** Staining for mitotic spindles in a mitotic cell (metaphase) in H^{-/-};ErbB2 mouse mammary tumor (a and e). Nuclear staining (DAPI), (b and f) centrosomes (γ -Tubulin), (c and g) mitotic spindles (α -Tubulin), (d and h) merge. (a-d) a mitotic cell with normal (2) spindle poles and 2 centrosomes. (e-h) a mitotic cell with no centrosomes (acentrosomal) and abnormal (>2) spindle poles. Arrows point to the position of the centrosomes in the mitotic cell. Asterisks indicate the 3 directions of the pull of the acentrosomal spindle poles.

Indeed, we observed acentrosomal polar spindles in mammary tumors of p53^{H/-} mice. Fig. 7F (upper panels) show an example of a normal mitotic cell with two centrosomes and two polar spindles, while Fig. 7F (lower

panels) demonstrate an example of an abnormal mitotic cell with centrosomes absent and three polar spindles. No acentrosomal mitotic cells were detected in the p53^{+/+}, p53^{-/+}, p53^{-/-} and p53^{H/+} mammary tumors.

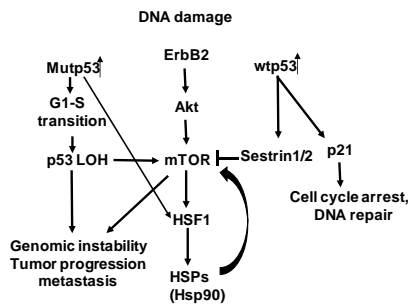


Fig. 8. Molecular mechanisms of p53 loss of heterozygosity in breast cancer in response to DNA damage. Proposed model.

Collectively our data suggest that under normal condition, transcriptionally competent *wtp53* allele enables the genomic integrity and suppresses the mTOR pathway in *mutp53* heterozygous ErbB2 cancer cells. As an early response in *mutp53* heterozygous cells, genotoxic stress promotes sustained *mutp53* stabilization, continuous DNA damage, and aberrant G1-S transition. The deficient cell cycle checkpoint coupled with inefficiently repaired DNA leads to a higher

frequency of p53LOH, mTOR upregulation and higher genomic instability in *mutp53* heterozygous cells. After p53LOH, *mutp53* through amplification of HSF1 activity can further stimulate the mTOR pathway, whereby enhancing cancer cells fitness and enabling tumor progression. Contrary, *wtp53* allele in p53^{-/+};ErbB2 and p53^{+/+};ErbB2 cells induces growth arrest and, inhibits the mTOR activity via induction of p21 and sestrin2 respectively (Fig. 8).

Major Task 3. Determine whether p53 LOH promotes metastatic behavior in ErbB2 cancer cells.

Subtask 1. Establish whether p53 LOH enhances the motility and invasion of cancer cells in vitro.

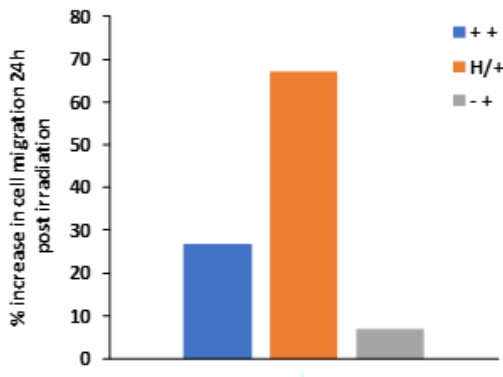


Fig.9 Mutp53 allele promotes migration in heterozygous cells after irradiation. Cells were γ -irradiated (9Gy), or not, and 24h post-irradiation were assayed for migration using transwell assay. Cells were fixed and stained using crystal violet. Cell were counted in 4 random fields per treatment. For each cell genotype, the percent change in cell migration post irradiation as compared to non-irradiated

Test the motility and invasive properties of primary mammary epithelial cells and tumor cultures derived from H/+;ErbB2 and p53^{-/+};ErbB2 mice before and after LOH in vitro. Boyden chamber assay, wound healing assay, metastases in allografts. (timeline: months 24-32, 20% completion). First, we assessed the short-term (p53LOH independent) effect of irradiation on cells motility in context of p53 genotype. We tested migration 24h after irradiation. At this time point we observed only marginal loss of *wtp53* allele in H/+;ErbB2 cells (Fig. 4B). Strikingly, we found that irradiation induces migration in all genotypes, but more profoundly in H/+;ErbB2 cells (Fig. 9). Therefore, p53LOH-independent effects may contribute to motility after irradiation. We hypothesized that irradiation-induced

mutp53 stabilization (Fig. 1C) may impose *mutp53* dominant-negative effect over *wtp53* allele, inducing metastases that we observed *in vivo*. The dramatic difference in motility between H/+;ErbB2 and -/+;ErbB2 after irradiation (Fig. 9) supports this hypothesis. To identify pathways involved in an increase in the motility,

currently we are performing the RNAseq analysis of cells with different genotypes, which were irradiated (24h) or not. RNA samples will be analyzed by Novogene (Chula Vista, CA, USA). We expect to receive the results of this experiment in 20 days. Although beyond the scope of the proposed subtask, this data will provide us the valuable mechanistic insight of how mutp53 induces metastases *in vivo* and identify potentially druggable targets, which will help to alleviate potentially detrimental effects of radiotherapy at early stages of breast cancer.

To determine the long-term effect of irradiation in context of p53LOH, we will continue these experiments 10 days after irradiation to correlate p53LOH and motility, when we observed a significant increase in p53 LOH in H+;ErbB2 cells (Fig. 4B).

Subtask 2. Determine whether p53 LOH enhances the ability of tumor cells to metastasize in vivo. Isolate metastatic cells from lungs of irradiated and non-irradiated of R172H+;ErbB2 vs. p53-/+;ErbB2 vs. p53+/+;ErbB2 mice. Assess p53 LOH status in metastases in comparison with primary tumors. (timeline: months 24-32, 0% completion).

- 1 Li, D., Yallowitz, A., Ozog, L. & Marchenko, N. A gain-of-function mutant p53-HSF1 feed forward circuit governs adaptation of cancer cells to proteotoxic stress. *Cell Death Dis* **5**, e1194, doi:10.1038/cddis.2014.158 (2014).
- 2 Yallowitz, A. R. *et al.* Mutant p53 Amplifies Epidermal Growth Factor Receptor Family Signaling to Promote Mammary Tumorigenesis. *Mol Cancer Res* **13**, 743-754, doi:10.1158/1541-7786.MCR-14-0360 (2015).
- 3 Alexandrova, E. M. *et al.* p53 loss-of-heterozygosity is a necessary prerequisite for mutant p53 stabilization and gain-of-function in vivo. *Cell Death Dis* **8**, e2661, doi:10.1038/cddis.2017.80 (2017).
- 4 Alexandrova, E. M. *et al.* Improving survival by exploiting tumour dependence on stabilized mutant p53 for treatment. *Nature* **523**, 352-356, doi:10.1038/nature14430 (2015).
- 5 Bug, M. & Dobbelstein, M. Anthracyclines induce the accumulation of mutant p53 through E2F1-dependent and -independent mechanisms. *Oncogene* **30**, 3612-3624, doi:10.1038/onc.2011.72 (2011).
- 6 Leonard, M. K., Hill, N. T., Bubulya, P. A. & Kadakia, M. P. The PTEN-Akt pathway impacts the integrity and composition of mitotic centrosomes. *Cell Cycle* **12**, 1406-1415, doi:10.4161/cc.24516 (2013).
- 7 Aoki, K., Tamai, Y., Horiike, S., Oshima, M. & Taketo, M. M. Colonic polyposis caused by mTOR-mediated chromosomal instability in Apc+/Delta716 Cdx2+/- compound mutant mice. *Nat Genet* **35**, 323-330, doi:10.1038/ng1265 (2003).
- 8 Ghaleb, A. M., Elkarim, E. A., Bialkowska, A. B. & Yang, V. W. KLF4 Suppresses Tumor Formation in Genetic and Pharmacological Mouse Models of Colonic Tumorigenesis. *Mol Cancer Res* **14**, 385-396, doi:10.1158/1541-7786.MCR-15-0410 (2016).
- 9 Wang, X. *et al.* Overexpression of aurora kinase A in mouse mammary epithelium induces genetic instability preceding mammary tumor formation. *Oncogene* **25**, 7148-7158, doi:10.1038/sj.onc.1209707 (2006).
- 10 Schulz, R. *et al.* HER2/ErbB2 activates HSF1 and thereby controls HSP90 clients including MIF in HER2-overexpressing breast cancer. *Cell Death Dis* **5**, e980, doi:10.1038/cddis.2013.508 (2014).
- 11 Chou, S. D., Prince, T., Gong, J. & Calderwood, S. K. mTOR is essential for the proteotoxic stress response, HSF1 activation and heat shock protein synthesis. *PLoS One* **7**, e39679, doi:10.1371/journal.pone.0039679 (2012).
- 12 Budanov, A. V. & Karin, M. p53 target genes sestrin1 and sestrin2 connect genotoxic stress and mTOR signaling. *Cell* **134**, 451-460, doi:10.1016/j.cell.2008.06.028 (2008).

- 13 Vadysirisack, D. D., Baenke, F., Ory, B., Lei, K. & Ellisen, L. W. Feedback control of p53 translation by REDD1 and mTORC1 limits the p53-dependent DNA damage response. *Mol Cell Biol* **31**, 4356-4365, doi:10.1128/MCB.05541-11 (2011).
- 14 Hanel, W. & Moll, U. M. Links between mutant p53 and genomic instability. *J Cell Biochem* **113**, 433-439, doi:10.1002/jcb.23400 (2012).
- 15 Yang, K., Hitomi, M. & Stacey, D. W. Variations in cyclin D1 levels through the cell cycle determine the proliferative fate of a cell. *Cell Div* **1**, 32, doi:10.1186/1747-1028-1-32 (2006).
- 16 Hitomi, M. & Stacey, D. W. Cyclin D1 production in cycling cells depends on ras in a cell-cycle-specific manner. *Curr Biol* **9**, 1075-1084 (1999).
- 17 Hitomi, M. & Stacey, D. W. Cellular ras and cyclin D1 are required during different cell cycle periods in cycling NIH 3T3 cells. *Mol Cell Biol* **19**, 4623-4632 (1999).
- 18 Blagosklonny, M. V. & Pardee, A. B. The restriction point of the cell cycle. *Cell Cycle* **1**, 103-110 (2002).
- 19 Musacchio, A. & Salmon, E. D. The spindle-assembly checkpoint in space and time. *Nat Rev Mol Cell Biol* **8**, 379-393, doi:10.1038/nrm2163 (2007).
- 20 Rao, C. V. & Yamada, H. Y. Genomic instability and colon carcinogenesis: from the perspective of genes. *Front Oncol* **3**, 130, doi:10.3389/fonc.2013.00130 (2013).
- 21 Lane, D. & Levine, A. p53 Research: the past thirty years and the next thirty years. *Cold Spring Harb Perspect Biol* **2**, a000893, doi:10.1101/cshperspect.a000893 (2010).
- 22 Linke, S. P. *et al.* p53 interacts with hRAD51 and hRAD54, and directly modulates homologous recombination. *Cancer Res* **63**, 2596-2605 (2003).
- 23 Menon, V. & Povirk, L. Involvement of p53 in the repair of DNA double strand breaks: multifaceted Roles of p53 in homologous recombination repair (HRR) and non-homologous end joining (NHEJ). *Subcell Biochem* **85**, 321-336, doi:10.1007/978-94-017-9211-0_17 (2014).
- 24 Akyuz, N. *et al.* DNA substrate dependence of p53-mediated regulation of double-strand break repair. *Mol Cell Biol* **22**, 6306-6317 (2002).
- 25 Lin, Y., Waldman, B. C. & Waldman, A. S. Suppression of high-fidelity double-strand break repair in mammalian chromosomes by pifithrin-alpha, a chemical inhibitor of p53. *DNA Repair (Amst)* **2**, 1-11 (2003).
- 26 Rodgers, K. & McVey, M. Error-Prone Repair of DNA Double-Strand Breaks. *J Cell Physiol* **231**, 15-24, doi:10.1002/jcp.25053 (2016).
- 27 Chin, K. *et al.* In situ analyses of genome instability in breast cancer. *Nat Genet* **36**, 984-988, doi:10.1038/ng1409 (2004).
- 28 Ghadimi, B. M. *et al.* Centrosome amplification and instability occurs exclusively in aneuploid, but not in diploid colorectal cancer cell lines, and correlates with numerical chromosomal aberrations. *Genes Chromosomes Cancer* **27**, 183-190 (2000).
- 29 Lingle, W. L. *et al.* Centrosome amplification drives chromosomal instability in breast tumor development. *Proc Natl Acad Sci U S A* **99**, 1978-1983, doi:10.1073/pnas.032479999 (2002).
- 30 Pihan, G. A. *et al.* Centrosome defects and genetic instability in malignant tumors. *Cancer Res* **58**, 3974-3985 (1998).
- 31 Pihan, G. A., Wallace, J., Zhou, Y. & Doxsey, S. J. Centrosome abnormalities and chromosome instability occur together in pre-invasive carcinomas. *Cancer Res* **63**, 1398-1404 (2003).
- 32 Fukasawa, K., Choi, T., Kuriyama, R., Rulong, S. & Vande Woude, G. F. Abnormal centrosome amplification in the absence of p53. *Science* **271**, 1744-1747 (1996).
- 33 Tarapore, P. & Fukasawa, K. Loss of p53 and centrosome hyperamplification. *Oncogene* **21**, 6234-6240, doi:10.1038/sj.onc.1205707 (2002).
- 34 Tarapore, P., Horn, H. F., Tokuyama, Y. & Fukasawa, K. Direct regulation of the centrosome duplication cycle by the p53-p21Waf1/Cip1 pathway. *Oncogene* **20**, 3173-3184, doi:10.1038/sj.onc.1204424 (2001).
- 35 Shinmura, K., Bennett, R. A., Tarapore, P. & Fukasawa, K. Direct evidence for the role of centrosomally localized p53 in the regulation of centrosome duplication. *Oncogene* **26**, 2939-2944, doi:10.1038/sj.onc.1210085 (2007).

- What opportunities for training and professional development has the project provided?

Malik Padellan, undergraduate student, Stony Brook University (September 2018-), and Boris Nekrasov (June18-August18, high school student) have received professional on-hand training while working on this project.

- How were the results disseminated to communities of interest?

Oral presentations:

1) Stony Brook University Pathology Grand rounds (5/31/2018): Molecular mechanisms of p53 deregulation in HER2-positive breast cancer in response to radiation.

2) VA, Northport Medical Center, NY, "Lunch and Learn" seminar series for medical residents (9/21/2018): P53 LOH in HER2-positive breast cancer in response to radiation: possible driver(s).

- What do you plan to do during the next reporting period to accomplish the goals?

For the next reporting period we will continue experiments described in Major Task 1 Subtask 3,4 to determine the effect of doxorubicin and irradiation on p53LOH in the neoadjuvant setting. We will also focus on the implementation of Major Task 3 to determine 1) whether p53LOH in the presence of mutp53 allele promotes metastases in vivo and in vitro; 2) the mechanism, by which mutp53 promotes metastases in ErbB2-driven breast cancer in context of p53 LOH.

4.IMPACT

- Major innovative findings and achievements for this reporting period:

1) Using MMTV;ErbB2 mouse model carrying heterozygous R172H p53 mutation, we show that under normal condition, transcriptionally competent wtp53 allele enables the genomic integrity and suppresses the mTOR pathway in mutp53 heterozygous ErbB2 cancer cells; 2) In the long run, the single dose of irradiation of premalignant lesions accelerates mammary tumorigenesis, induces p53LOH and metastases that are more profound in the presence of mutant p53 allele; 3) As an early response in mutant p53 heterozygous cells, genotoxic stress promotes sustained mutant p53 stabilization, continuous DNA damage, and aberrant G1-S transition; 4) Mechanistically, the deficient cell cycle checkpoint coupled with inefficiently repaired DNA underlies the higher frequency of p53LOH in mutant p53 heterozygous cells; 5) The main physiological

outcomes of p53LOH are profound stabilization of mutant p53 protein, mTOR upregulation, enhanced genomic instability, and metastases.

Collectively, our results imply that in mutant p53 heterozygous cells, genotoxic stress facilitates the selective pressure for wtp53 loss. The latter enhances cancer cells fitness by mTOR upregulation and provides the genetic plasticity for the acquisition of metastatic properties.

- What was the impact on the development of the principal discipline(s) of the project?

We completed the study, where we utilized mouse model and cell lines generated for awarded study (Yallowitz A, Ghaleb A, Garcia L, Alexandrova E, Marchenko N. Heat Shock Factor 1 confers resistance to lapatinib in ErbB2 positive breast cancer cells. 2018, Cell Death Dis., 2018 May 24;9(6):621. doi: Cell Death and Disease (impact factor 5,965). The second manuscript that summarized the results described above will be submitted within two weeks to Nature Communications.

- What was the impact on other disciplines?

Nothing to Report.

- What was the impact on technology transfer?

Nothing to Report.

- What was the impact on society beyond science and technology?

Nothing to Report.

5. CHANGES/PROBLEMS:

As we described above, we encountered problem with the scoring of IHC staining for the implementation of Major Task1 Subtask 1, as ErbB2 staining produced overwhelmingly strong signal, while HSF1 staining was low and unspecific in mouse tumor tissues. To overcome these problems, we switched to analysis of mTOR that is a major downstream signaling target of ErbB2 and utilized in vitro studies to address genotype-specific effect of p53LOH on HSF1 signaling. In both cases, the alternative approaches helped us to solve initial problems.

- Significant changes in use or care of human subjects, vertebrate animals, biohazards, and/or select agents

Nothing to Report.

- Significant changes in use or care of human subjects

Nothing to Report.

- Significant changes in use or care of vertebrate animals.

Nothing to Report.

- Significant changes in use of biohazards and/or select agents

Nothing to Report.

6. PRODUCTS:

Journal publications.

Yallowitz A, Ghaleb A, Garcia L, Alexandrova E, Marchenko N. Heat Shock Factor 1 confers resistance to lapatinib in ErbB2 positive breast cancer cells. 2018, Cell Death Dis., 2018 May 24;9(6):621. doi: 10.1038/s41419-018-0691-x.

Ghaleb A., Yallowitz A, Marchenko N. "Irradiation augments p53 loss of heterozygosity in ErbB2-driven mammary tumors". The manuscript is in preparation.

Both publications contain acknowledgement of DOD support.

Other Products

Oral presentations:

- 1) Stony Brook University Pathology Grand rounds (5/31/2018): Molecular mechanisms of p53 deregulation in HER2-positive breast cancer in response to radiation.
- 2) VA, Northport Medical Center, NY, "Lunch and Learn" seminar series for medical residents (9/21/2018): P53 LOH in HER2-positive breast cancer in response to radiation: possible driver(s).

7. PARTICIPANTS & OTHER COLLABORATING ORGANIZATIONS

Has there been a change in the active other support of the PD/PI(s) or senior/key personnel since the last reporting period?

Name:	Natalia Marchenko
Project Role:	PI
Researcher Identifier (e.g. ORCID ID):	
Nearest person month worked:	12 months
Contribution to Project:	Dr. Marchenko was responsible for the overall administration, data analysis, coordination and direction of the project and lab work. Dr. Marchenko performed breeding and mouse colony maintenance, tumor specimens analysis, mammary epithelial cells isolation, manuscript preparation.
Funding Support:	DOD # BC151569
Name:	Euvgenia Alexandrova
Project Role:	Collaborator
Researcher Identifier (e.g. ORCID ID):	
Nearest person month worked:	3 months
Contribution to Project:	As a collaborator Dr. Alexandrova was involved in generation, specimen tissue preparation and data analysis of R248Q;ErbB2 mice, manuscript preparation.
Funding Support:	NCI gran t# K22CA190653-01A1
Name:	Amr Ghaleb
Project Role:	investigator

Researcher Identifier (e.g. ORCID ID):	
Nearest person month worked:	12 months
Contribution to Project:	Amr was responsible for breeding and mouse colony maintenance, mouse genotyping, performed tissue embedding, cutting and IHC staining, QRT-PCR, in vitro experiments.
Funding Support:	
Name:	Malik Padellan
Project Role:	Undergraduate Student, Stony Brook University
Researcher Identifier (e.g. ORCID ID):	
Nearest person month worked:	1 months
Contribution to Project:	Malik performed Western blot analysis of cell lines, mice genotyping and assessment of p53 LOH status in cell lines.
Funding Support:	none
Name:	
Project Role:	
Researcher Identifier (e.g. ORCID ID):	
Nearest person month worked:	2 months
Contribution to Project:	
Funding Support:	
Name:	Ute Moll

Project Role:	Collaborator
Researcher Identifier (e.g. ORCID ID):	
Nearest person month worked:	1 month
Contribution to Project:	As a collaborator Dr. Moll participated in planning of experiments, discussions of data interpretations, manuscript preparation.
Funding Support:	NCI grant R01CA176647

- What other organizations were involved as partners?

Nothing to Report

8. SPECIAL REPORTING REQUIREMENTS

Nothing to Report

ARTICLE

Open Access

Heat shock factor 1 confers resistance to lapatinib in ERBB2-positive breast cancer cells

Alisha Yallowitz^{1,2}, Amr Ghaleb¹, Lucas Garcia¹, Evguenia M. Alexandrova¹ and Natalia Marchenko¹

Abstract

Despite success of ERBB2-targeted therapies such as lapatinib, resistance remains a major clinical concern. Multiple compensatory receptor tyrosine kinase (RTK) pathways are known to contribute to lapatinib resistance. The heterogeneity of these adaptive responses is a significant hurdle for finding most effective combinatorial treatments. The goal of this study was to identify a unifying molecular mechanism whose targeting could help prevent and/or overcome lapatinib resistance. Using the MMTV-ERBB2;mutant p53 (R175H) in vivo mouse model of ERBB2-positive breast cancer, together with mouse and human cell lines, we compared lapatinib-resistant vs. lapatinib-sensitive tumor cells biochemically and by kinome arrays and evaluated their viability in response to a variety of compounds affecting heat shock response. We found that multiple adaptive RTKs are activated in lapatinib-resistant cells in vivo, some of which have been previously described (Axl, MET) and some were novel (PDGFR α , PDGFR β , VEGFR1, MUSK, NFGFR). Strikingly, all lapatinib-resistant cells show chronically activated HSF1 and its transcriptional targets, heat shock proteins (HSPs), and, as a result, superior tolerance to proteotoxic stress. Importantly, lapatinib-resistant tumors and cells retained sensitivity to Hsp90 and HSF1 inhibitors, both in vitro and in vivo, thus providing a unifying and actionable therapeutic node. Indeed, HSF1 inhibition simultaneously downregulated ERBB2, adaptive RTKs and mutant p53, and its combination with lapatinib prevented development of lapatinib resistance in vitro. Thus, the kinome adaptation in lapatinib-resistant ERBB2-positive breast cancer cells is governed, at least in part, by HSF1-mediated heat shock pathway, providing a novel potential intervention strategy to combat resistance.

Introduction

Human epidermal growth factor receptor 2 (Her2, ERBB2) is overexpressed in about 25% of sporadic human breast cancer cases, which correlates with poor prognosis¹. Several ERBB2-targeted therapies are currently available that improve patients' outcomes, including a dual ERBB2/EGFR kinase inhibitor lapatinib². However, acquired resistance to lapatinib remains a major concern for its clinical utilization.

Multiple mechanisms of lapatinib resistance are described in the literature. They primarily involve compensatory activation of receptor tyrosine kinases (RTKs), such as ERBB3, IGF1R, MET, FGFR2, FAK, Axl, as well as other mechanisms². Importantly, not a single, but multiple RTKs have been shown to be activated in response to lapatinib³. Also, the substantial heterogeneity among adaptive RTKs exists in different cell lines in response to lapatinib³. This represents a major hurdle for the development of successful combinatorial strategies to reverse and/or prevent lapatinib resistance. Hence, identification and targeting of an upstream effector governing the kinome adaptation in response to ERBB2 inhibition would help to overcome this clinical dilemma.

Correspondence: Natalia Marchenko (natalia.marchenko@stonybrook.edu)

¹Department of Pathology, Stony Brook University, Stony Brook, NY 11794-8691, USA

²Weill Cornell Medicine, 1300 York Avenue, LC-902, New York, NY 10065, USA

Edited by R. Aqelani

© The Author(s) 2018



Open Access This article is licensed under a Creative Commons Attribution 4.0 International License, which permits use, sharing, adaptation, distribution and reproduction in any medium or format, as long as you give appropriate credit to the original author(s) and the source, provide a link to the Creative Commons license, and indicate if changes were made. The images or other third party material in this article are included in the article's Creative Commons license, unless indicated otherwise in a credit line to the material. If material is not included in the article's Creative Commons license and your intended use is not permitted by statutory regulation or exceeds the permitted use, you will need to obtain permission directly from the copyright holder. To view a copy of this license, visit <http://creativecommons.org/licenses/by/4.0/>.

Our previous studies identified heat shock factor 1 (HSF1) as a key effector of ERBB2 signaling^{4–6}. HSF1 is a transcription factor that controls a broad spectrum of pro-survival events essential for protecting cells from proteotoxic stress, which is caused by the accumulation of misfolded proteins in cancer cells. HSF1 activates transcription of genes that regulate protein homeostasis, including heat shock proteins (HSPs), Hsp27, Hsp70, and Hsp90⁷, as well as supports other oncogenic processes such as cell cycle regulation, metabolism, adhesion, and protein translation^{8, 9}. The impact of HSF1 on ERBB2-driven mammary tumorigenesis was unequivocally proven by *in vivo* studies. The genetic ablation of HSF1 suppresses mammary hyperplasia and reduces tumorigenesis in ERBB2 transgenic mice¹⁰. Consistently, the stability of ERBB2 protein is shown to be maintained by transcriptional targets of HSF1: Hsp70, Hsp90¹¹, and Hsp27⁷.

Mutations in the *TP53* gene (*mutp53*) are the most frequent genetic events in ERBB2-positive breast cancer (72%)¹² and correlate with poor patient outcomes¹³. To recapitulate human ERBB2-positive breast cancer in mice, we previously generated a novel mouse model that combines activated ERBB2 (MMTV-ERBB2 allele¹⁴) with the *mutp53* allele R172H corresponding to human hotspot *mutp53* allele R175H¹². We found that *mutp53* accelerates ERBB2-driven mammary tumorigenesis¹⁵. The underlying molecular mechanism is a *mutp53*-driven oncogenic feed-forward loop governing a superior survival of cancer cells. We found that *mutp53*, through enhanced recycling and/or stability of ERBB2/EGFR, augments MAPK and PI3K signaling, leading to transcriptional phospho-activation of HSF1 at Ser326. Furthermore, *mutp53* directly interacts with phospho-activated HSF1 and facilitates its binding to DNA-response elements, thereby stimulating transcription of HSPs⁵. In turn, HSPs more potently stabilize their oncogenic clients ERBB2, EGFR, *mutp53*, HSF1, thus reinforcing tumor development⁵. Consistently, we found that lapatinib not only suppresses tumor progression, but does so, at least in part, via inactivation of HSF1¹⁵. Furthermore, the interception of the ERBB2-HSF1-*mutp53* feed-forward loop by lapatinib destabilizes *mutp53* protein in Hsp90-dependent and Mdm2-dependent manner⁴. Since *mutp53* ablation has been shown to have therapeutic effects *in vivo*¹⁶, it is possible that *mutp53* destabilization by lapatinib contributes to its anti-cancer activity.

In the present study, we identified HSF1 as an important upstream node responsible for the kinome adaptation of lapatinib-resistant cells. We found that lapatinib-resistant cancer cells have enhanced HSF1 activity, a superior resistance to proteotoxic stress, and lose their ability to degrade *mutp53* in response to lapatinib. In contrast, HSF1 inhibition blocks lapatinib-induced kinome

adaptation and prevents the development of lapatinib resistance. Our data suggest a mechanism-based rationale for the clinical utilization of HSF1 inhibitors for the treatment of lapatinib-resistant ERBB2-positive breast cancer and/or—in combination with lapatinib—to prevent development of lapatinib resistance.

Results

Generation and characterization of human and mouse lapatinib-resistant ERBB2-positive breast cancer cell lines

To gain the mechanistic insight into lapatinib resistance we utilized two complementary approaches: *in vitro* and *in vivo*. For *in vitro* studies, we continuously cultivated human ERBB2-positive BT474 breast cancer cells in the presence of increasing concentrations (100–300 nM) of lapatinib for 6 months. All selected lapatinib-resistant clones were combined and maintained as a pool, as previously described³. Lapatinib-resistant cells approximately doubled their viability compared to lapatinib-sensitive cells (Fig. 1a), which was associated with decreased apoptosis in the presence of lapatinib (Fig. 1b).

To investigate lapatinib resistance acquired *in vivo*, we utilized the previously described MMTV-ERBB2;R172H mouse model of ERBB2-positive breast cancer (“R172H/+;ERBB2” hereafter)¹⁵. At the age of mammary microlesions (8-weeks old), R172H/+;ERBB2 females were given lapatinib (75 mg/kg three times a week) or vehicle by oral gavage, lifelong. Consistent with human data, lapatinib shows a tendency to delay tumor onset (from 256 to 319 days, median onset, $p = 0.091$) and significantly extended overall survival (from 321 to 362 days, median survival, $p = 0.014$) compared to vehicle-treated mice (Fig. 1c). However, after initial response (Fig. 1c) mammary tumors acquired lapatinib resistance and started to exhibit growth kinetics similar to vehicle-treated tumors (Fig. 4a).

We established cell lines from both vehicle-treated (lapatinib-sensitive; 1349, 1347, 1251, 1252, 1253) and lapatinib-treated (lapatinib-resistant; 125R) mouse mammary tumors. In contrast to previous studies using human ERBB2-positive breast cancer cell lines³, our murine cell lines were derived from littermates, have an identical genetic background, the same mutation and acquired lapatinib resistance *in vivo* (with normal gland architecture, tumor microenvironment, immune system status), and therefore should better reflect the resistance mechanisms encountered in patients in the clinic. The short-term cell viability assay and the long-term colony formation assays both confirmed that the established cell lines continued to maintain their lapatinib resistance acquired *in vivo* (Fig. 1d, e).

To test for possible compensatory mechanisms induced *in vivo*, we performed the kinome profiling of 39 activated

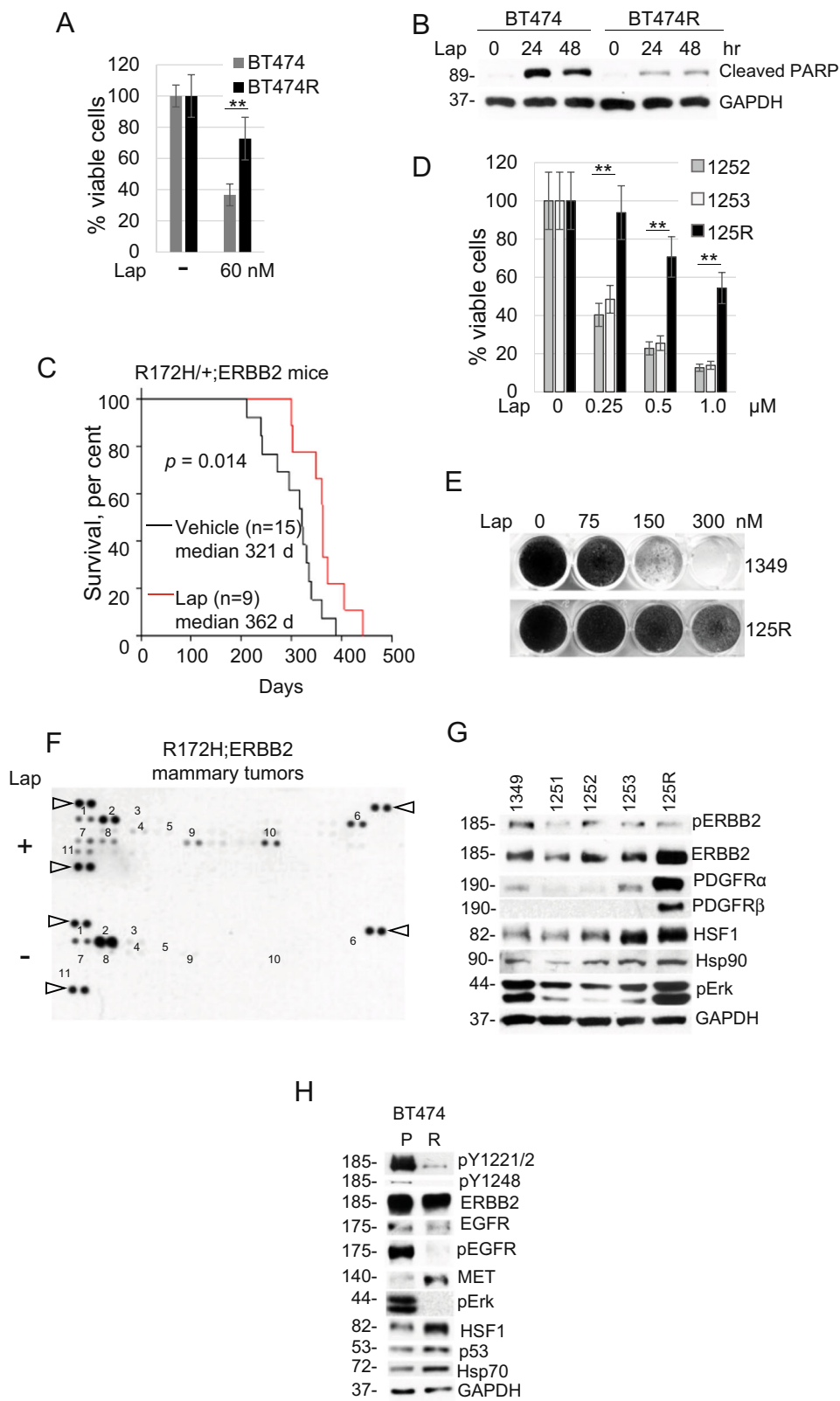


Fig. 1 (See legend on next page.)

(see figure on previous page)

Fig. 1 Generation and characterization of lapatinib-resistant human and mouse Her2-positive cancer cell lines. **a, b** Lapatinib-resistant human BT474R cells exhibit a two-fold increased viability after 48 h treatment with lapatinib (**a**) and a significantly decreased apoptosis after treatment with 300 nM lapatinib for indicated times (measured by cleaved PARP, **b**) compared to lapatinib-sensitive parental BT474 cells. **b** Western blot analysis, GAPDH is a loading control. One representative experiment out of two independent experiments (each performed in triplicate) is shown; $**p < 0.01$ for three technical replicas, Student's *t*-test (**a, b**). **c** Tumor onset is significantly delayed in R172H/+;ERBB2 females treated with 75 mg/kg lapatinib three times a week starting at 8 weeks of age lifelong (red line) compared to vehicle-treated siblings (black line). Kaplan–Meier analysis, log rank statistics. **d, e** Murine primary cell lines established from lapatinib-sensitive mammary tumors (1252, 1253, 1349) and from a lapatinib-resistant mammary tumor (125R) maintain lapatinib sensitivity and lapatinib resistance in vitro, respectively. **d** Short-term cell viability assay (48 h). One representative experiment out of two independent experiments (each performed in triplicate) is shown; $**p < 0.01$ for three technical replicas, Student's *t*-test. **e** Long-term colony formation assay (4 weeks). **f** Lapatinib induces activation of multiple adaptive RTKs in vivo. Representative images of the mouse Phospho-RTK array kit comparing lapatinib-treated (i.e., lapatinib-resistant, top) with vehicle-treated (i.e., lapatinib-sensitive, bottom) tumors. 1. EGFR*, 2. ERBB2*, 3. ERBB3, 4. PDGFR α *, 5. PDGFR β *, 6. Axl*, 7. NGFR, 8. VEGFR1*, 9. MUSK*, 10. EPHA2*, 11. EPHB2. Known Hsp90 clients are marked with an asterisk. Triangles mark reference spots. **g, h** Murine lapatinib-resistant 125R cells show upregulated PDGFR α and PDGFR β compared to murine lapatinib-sensitive cells 1349, 1251, 1252, 1253 (**g**), while human lapatinib-resistant BT474R cells have upregulated MET and downregulated ErbB2 and EGFR signaling (measured by phospho-ERBB2 pY1221/2 and pY1248, two top panels, phospho-EGFR and their effector phospho-Erk), compared to parental BT474 cells (**h**). Note that both human and mouse lapatinib-resistant cells have upregulated HSF1 and its transcriptional targets Hsp90 (**g**) and Hsp70 (**h**). Western blot analysis, constitutive heat shock protein 70 (Hsc70) and GAPDH served as a loading control

RTKs in lapatinib-treated vs. vehicle-treated tumors, respectively. In lapatinib-treated tumors we found expected downregulation of phospho-activated ERBB2 and EGFR and upregulation of multiple compensatory RTKs (Fig. 1f), including previously described Axl² and novel RTKs, such as NGFR, MUSK, VEGFR1, PDGFR α , PDGFR β , EPHA2, and EPHB2 (Fig. 1f). These results suggest a robust kinome reprogramming and a switch to multiple alternative RTKs in lapatinib-resistant cells. Consistently, we observed enhanced phospho-Erk, a common downstream RTK effector, in lapatinib-resistant 125R murine cell line (Fig. 1g). We validated the arrays data by Western blot analysis of the cell lines established from murine mammary tumors. Consistent with the array, PDGFR α and PDGFR β were upregulated in lapatinib-resistant 125R cells compared to lapatinib-sensitive cells (Fig. 1g). Interestingly, in human lapatinib-resistant BT474 PDGFR α and PDGFR β were not upregulated, and, instead, MET was elevated (Fig. 1h). This difference likely reflects the heterogeneity in adaptive responses noted previously³.

Despite the distinct adaptive RTK response in mouse vs. human lapatinib-resistant cancer cells, notably, they share an important common feature, i.e., stabilized PDGFR α , PDGFR β , and MET that are maintained by Hsp90 (<https://www.picard.ch/downloads/Hsp90interactors.pdf>). Therefore, we hypothesized that HSF1-mediated heat shock response is causative to the observed adaptive RTKs upregulation in lapatinib-resistant cells. Indeed, this link is supported by the fact that six out of eight RTKs upregulated in lapatinib-resistant mammary tumors—Axl, VEGFR1, MUSK, PDGFR β , PDGFR α , EPHA2—are known Hsp90 clients (www.picard.ch/downloads/Hsp90interactors.pdf).

Lapatinib-resistant breast cancer cells are resistant to proteotoxic stress

To test whether HSF1-induced heat shock response is involved in the kinome adaptation of lapatinib-resistant cells, we compared their viability under the proteotoxic stress condition with lapatinib-sensitive cells. We found both the cells that acquired lapatinib resistance in vitro (Fig. 2a) and in vivo (Fig. 2b) to be more resistant to the proteotoxic stress induced by the proteasome inhibitor MG132 (Fig. 2c) and heat shock (Fig. 2d), which correlated with reduced apoptosis measured by PARP cleavage (Fig. 2c, d).

HSF1 reveals its protective role under proteotoxic stress via transcriptional activation of HSPs by transcriptionally active pSer326-HSF1. Indeed, upon proteotoxic stress induced by heat shock (Fig. 2e) and proteasome inhibition (Fig. 2f) lapatinib-resistant BT474 cells show a higher level of pSer326-HSF1. Since pSer326-HSF1 antibodies are human specific, we tested activity of pHSF1 in murine lapatinib-resistant 125R cells by the level of HSF1 transcriptional targets Hsp70 and Hsp90, and again found their significant upregulation upon proteotoxic stress induced by heat shock (Fig. 2g) and proteasome inhibition (Fig. 2h). These data indicate that lapatinib resistance correlates with augmented HSF1 function, and, as a result, with a superior tolerance to proteotoxic stress.

Lapatinib fails to modulate the ERBB2–HSF1–mutp53 axis in lapatinib-resistant breast cancer cells

Previously we showed that lapatinib destabilizes mutp53 via inhibition of HSF1 activity⁴. We now tested the effect of lapatinib on mutp53 levels in lapatinib-resistant BT474 cells (Fig. 3a) and found that lapatinib lost its ability to destabilize mutp53 even at higher doses (Fig. 3a), likely as a result of chronic HSF1 activity. Indeed, lapatinib did not

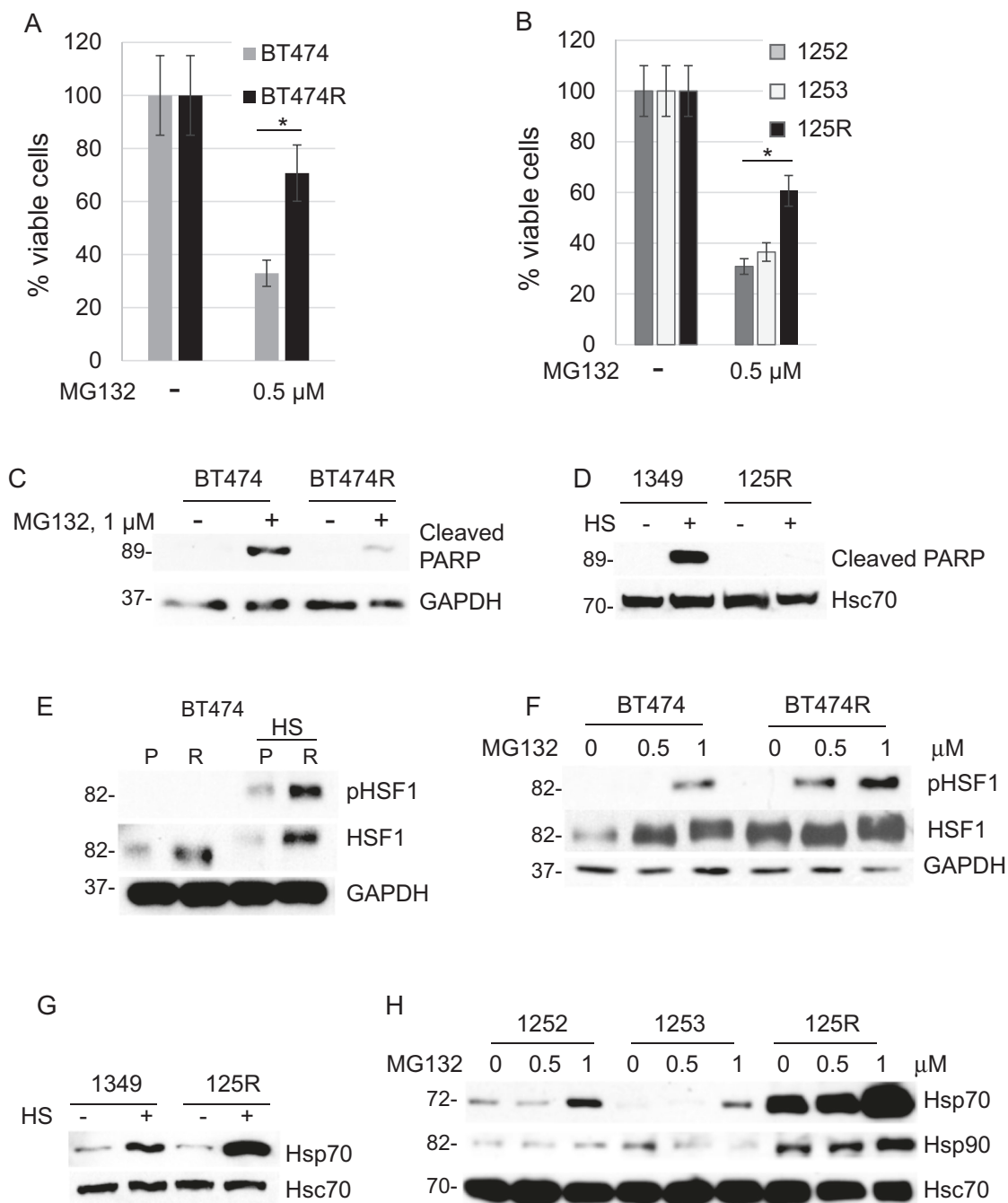
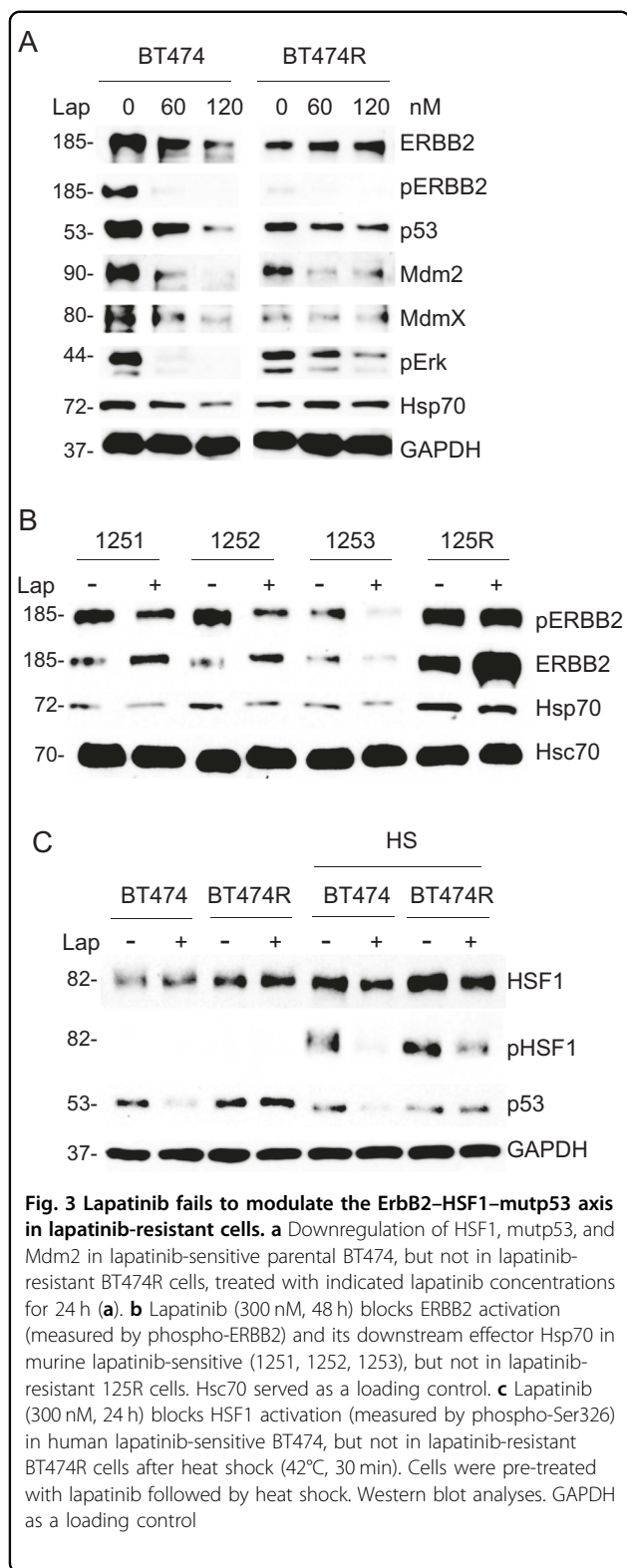


Fig. 2 Lapatinib-resistant cells are protected from proteotoxic stress. **a, b** Lapatinib-resistant human BT474R cells (**a**) and mouse 125R cells (**b**) are more resistant to proteotoxic stress induced by the proteasome inhibitor MG132 (0.5 μ M for 48 h) than their corresponding lapatinib-sensitive control cells. Cell viability assay. One representative experiment out of two independent experiments (each performed in triplicate) is shown; * $p < 0.05$ for three technical replicas, Student's *t*-test. **c–e** Under proteotoxic stress induced by (**c**) the proteasome inhibitor MG132 (1 μ M for 48 h) and (**d**) heat shock (43 C, 30 min, Western blot 48 h after) lapatinib-resistant human and murine cells have decreased apoptosis (cleaved PARP) and increased phospho-HSF1 (Ser326 **e, f**) compared to lapatinib-sensitive cells. Lapatinib-resistant murine 125R cells show upregulated heat shock protein Hsp70 to lapatinib-sensitive cells after proteotoxic stress induced by (**g**) heat shock (43 C, 30 min, Western blot 2 h after) and proteasome inhibitor MG132 (**h**). Western blot analysis. GAPDH and Hsc70 as a loading control



suppress HSF1 transcriptional target Hsp70, compared to lapatinib-sensitive cells, and failed to induce auto-degradation of Mdm2 and its bona fide substrates

MdmX and mutp53 (Fig. 3a). Since previous studies identified highly stabilized mutp53 protein as an essential pro-survival factor in cancer cells¹⁷, mutp53 depletion by lapatinib in lapatinib-sensitive cells could further enhance lapatinib's efficiency, while unresponsive high levels of mutp53 in lapatinib-resistant cells might contribute to the resistance mechanism. Similarly, lapatinib inhibited ERBB2 signaling (measured by phospho-ERBB2) and Hsp70 levels in sensitive murine lines, but failed to do so in the lapatinib-resistant murine 125R cells (Fig. 3b).

Proteotoxic stress induced by heat shock leads to transcriptional activation of HSF1 by Ser326 phosphorylation in both lapatinib-sensitive and resistant BT474 cells. However, lapatinib prevents phospho-activation of HSF1 after heat shock only in lapatinib-sensitive cells (Fig. 3c, compare lanes 5 and 6), but not in lapatinib-resistant BT474 cells (Fig. 3c, compare lanes 7 and 8). Most likely, HSF1 lost its dependency on the ERBB2 signaling in lapatinib-resistant cells due to the switch to alternative RTKs and their downstream effectors like Erk and Akt^{17, 18}, which reconstitutes HSF1 function and supports cells survival after ERBB2 inhibition¹⁹.

Altogether, these data reinforce that despite of the heterogeneity of adaptive responses, tumors acquire lapatinib resistance, at least in part, via unified HSF1-guided mechanism that feeds into stabilization of mutp53.

Lapatinib-resistant breast cancer cells are sensitive to Hsp90 inhibition

Since the majority of adaptive RTKs that we identified in vivo (Fig. 1f) are known Hsp90 clients, we hypothesized that lapatinib-resistant cells retain their sensitivity to Hsp90 inhibitors. To test this hypothesis, we used ganetespib, a new generation Hsp90 inhibitor, which is currently in several clinical trials²⁰. First, we tested the effect of ganetespib in vivo, using R172H/+;ERBB2 mice with mammary tumors that have been previously treated with lapatinib until they acquired resistance, i.e., lapatinib no longer suppressed their growth. Starting with the same average tumor size in each group, we designated three groups of animals (Fig. 4a): (i) animals previously treated with vehicle were continued on vehicle (Veh/Veh); (ii) animals previously treated with lapatinib (i.e., lapatinib-resistant) were continued on lapatinib alone (75 mg/kg three times a week lifelong) (Lap/Lap); (iii) some animals previously treated with lapatinib (i.e., lapatinib-resistant) were continued on lapatinib (75 mg/kg three times a week lifelong) together with ganetespib (50 mg/kg once a week lifelong) (Lap/Lap + Gan).

Consistently with their lapatinib resistance, the tumors on lapatinib alone continued to grow fast, with the rate very similar to vehicle-treated tumors (Fig. 4a, solid vs. small-dash lines). In contrast, addition of ganetespib significantly suppressed growth of lapatinib-resistant tumors

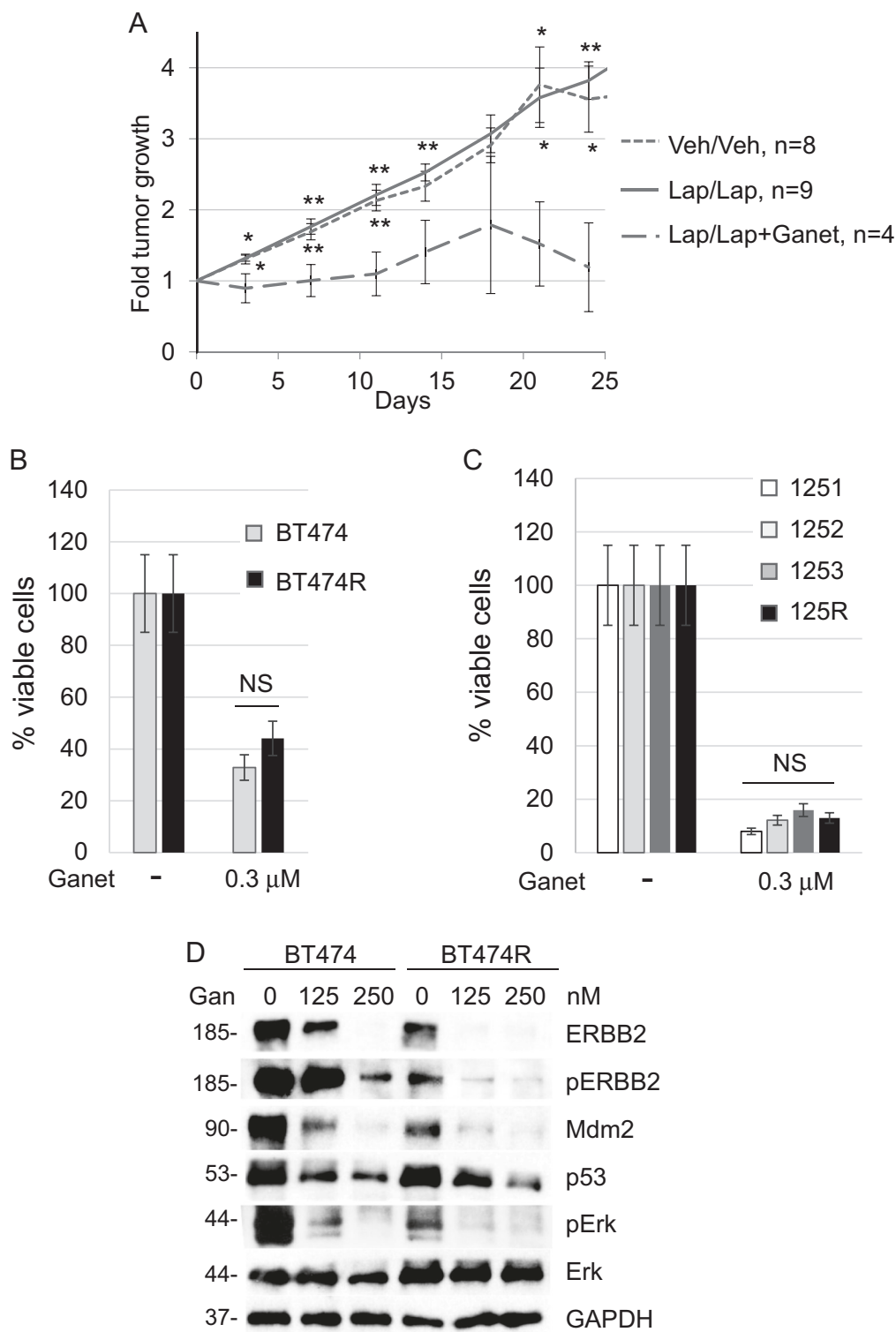


Fig. 4 (See legend on next page.)

(see figure on previous page)

Fig. 4 Lapatinib-resistant breast cancer cells are sensitive to Hsp90 inhibition. **a** R172H/+;ERBB2 female mice were treated either with vehicle or 50 mg/kg lapatinib (three times a week starting at 8 weeks of age) until tumors acquired lapatinib resistance, i.e., lapatinib no longer suppressed tumor growth. At this point, previously vehicle-treated mice were continued on vehicle (Veh/Veh), while previously lapatinib-treated mice continued to be treated with either lapatinib alone (Lap/Lap) or with lapatinib together with 50 mg/kg ganetespib once a week (Lap/Lap + Ganet), as described in Results. Note that the initial tumor size in all three groups was on average comparable. Tumor size was measured and plotted every 5 days. The treatment has been ended and mice were sacrificed when tumors in Veh/Veh and Lap/Lap arms reached the size of 3.5 cm³. Note that while lapatinib-resistant tumors grew similarly to untreated tumors (did not respond to lapatinib), addition of ganetespib significantly suppressed tumor growth (wide-dash line). * $p < 0.05$, ** $p < 0.01$, Student's *t*-test. Top asterisks compare the Lap/Lap + Ganet group with Lap/Lap, bottom asterisks compare the Lap/Lap + Ganet group with the Veh/Veh group. *n* number of independent tumors. **b, c** Lapatinib-sensitive human BT474 (**b**) and murine 125R (**c**) cells have similar sensitivity to ganetespib as their corresponding lapatinib-sensitive cells (BT474 and 1251, 1252, 1253, respectively). Cells were treated with DMSO or 0.3 μ M ganetespib for 48 h, followed by the cell viability assay. One representative experiment out of two independent experiments (each performed in triplicate) is shown; NS non-significant. **d** Ganetespib (indicated concentrations, 24 h) inhibits ERBB2 signaling (measured by phospho-ERBB2 and phospho-Erk) and destabilizes mutp53 and Mdm2 in both, lapatinib-sensitive BT474 and lapatinib-resistant BT474R cells. Western blot analysis, GAPDH is a loading control

(Fig. 4a, wide-dash vs. small-dash lines). These data demonstrate that, despite lapatinib and ganetespib having overlapping targets (ERBB2, EGFR, mutp53), ganetespib overcomes lapatinib-resistant adaptive responses and efficiently curbs growth of lapatinib-resistant tumors *in vivo*. Consistently with these *in vivo* data, both human and mouse lapatinib-resistant cell lines were highly sensitive to ganetespib *in vitro* (Fig. 4b, c). As expected, ganetespib effectively inhibited ERBB2 signaling (measured by phospho-ERBB2) and—contrary to lapatinib—depleted mutp53 and Mdm2 in both lapatinib-sensitive and lapatinib-resistant cells (Fig. 4d). We speculate that ganetespib suppresses growth of lapatinib-resistant tumors via two complementary mechanisms: targeting of compensatory RTKs and release Mdm2 from the Hsp90 inhibitory complex, leading to mutp53 degradation.

Hsf1 inhibition targets mutp53 and ERBB2 for degradation and suppresses growth of lapatinib-resistant breast cancer cells

Although Hsp90 inhibition seems to be an effective strategy to overcome lapatinib resistance, it has significant limitations. Hsp90 inhibitors have been shown to activate HSF1-mediated heat shock response, which in the long run protects cancer cells from apoptosis⁷.

Therefore, the efficacy of Hsp90 inhibitors is limited by HSF1 function. Thus, we set to test the effect of specific HSF1 inhibitor KRIBB11 (N2-(1H-indazole-5-yl)-N6-methyl-3-nitropyridine-2,6-diamine)²¹ on lapatinib-resistant vs. lapatinib-sensitive cells. Consistently with a previous report²², KRIBB11 inhibits HSF1 phosphorylation with or without proteotoxic stress (MG132) (Fig. 5a). As a readout of HSP suppression, KRIBB11 also dose-dependently suppressed Hsp90 clients ERBB2, mutp53 and Mdm2 in both lapatinib-sensitive and lapatinib-resistant human BT474 and mouse 125R cancer cells (Fig. 5b, c). Similarly, to Hsp90 inhibition by ganetespib

(Fig. 4d), KRIBB11 reactivated Mdm2 E3 ligase activity as manifested by downregulation of Mdm2 ubiquitination substrates MdmX, mutp53, and Mdm2 itself (Fig. 5b), which was rescued by the proteasome inhibitor MG132 (Fig. 5a, lanes 3, 4, Fig. 5d). These data indicate that HSF1 inhibition by KRIBB11 simultaneously targets both key oncogenic drivers, ERBB2 and mutp53, in lapatinib-sensitive and lapatinib-resistant ERBB2-overexpressing breast cancer cells. As a result, KRIBB11 dose-dependently kills lapatinib-sensitive and lapatinib-resistant human (Fig. 5e) and mouse (Fig. 5f) breast cancer cells with comparable efficiency.

Hsf1 inhibition suppresses adaptive RTK activation and overcome lapatinib resistance in ERBB2-positive breast cancer cells

Consistent with previous studies³, we noted a substantial heterogeneity of adaptive responses in lapatinib-resistant cancer cells, including RTKs such as MET³ and PDGFR α in human and mouse cells, respectively (Fig. 1). Interestingly, activation in response to lapatinib of both MET (Fig. 6a, b) and PDGFR α (Fig. 6c) occurred as quickly as 48 h after lapatinib treatment in lapatinib-resistant, as well as lapatinib-sensitive cells. It appears that it takes place at posttranscriptional level. RNAseq analysis of BT474 cells treated with lapatinib did not reveal induction of MET RNA transcript, while MET signaling was shown to be activated³. Since MET²² and PDGFR α ²³ are both Hsp90 clients, we asked if HSF1 inhibition by KRIBB11 would reverse MET and PDGFR α lapatinib-induced compensatory upregulation. Indeed, even the low KRIBB11 dose (1 μ M, compare to Fig. 5b, e) alleviated lapatinib-induced MET upregulation in both lapatinib-sensitive and lapatinib-resistant BT474 cells (Fig. 6a, b). Moreover, KRIBB11 synergized with lapatinib in degrading mutp53 and EGFR in lapatinib-sensitive BT474 cells (Fig. 6a) and restored mutp53 responsiveness to lapatinib in lapatinib-resistant BT474R cells (Fig. 6b).

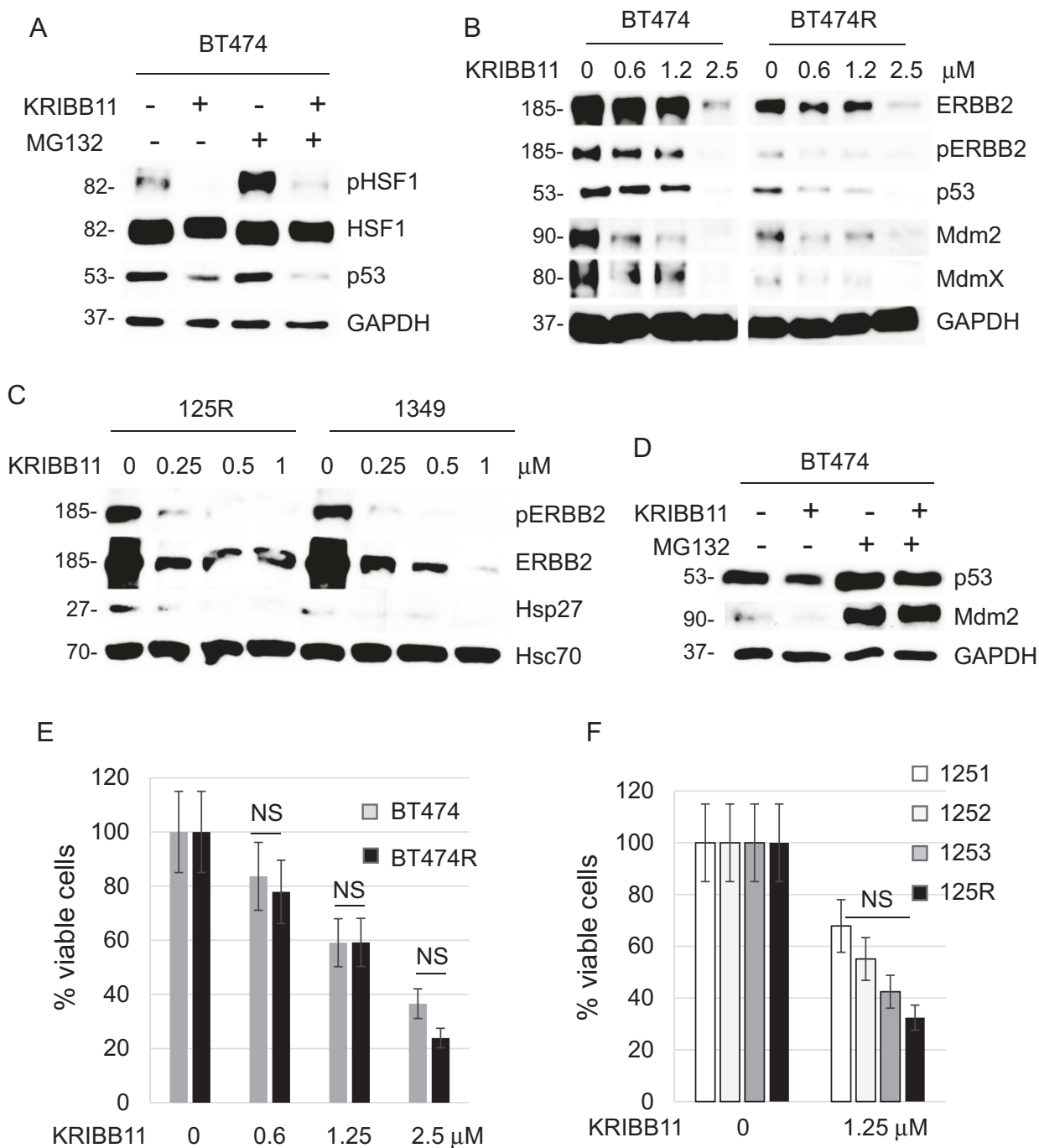


Fig. 5 HSF1 inhibition causes degradation of mutp53 and ErbB2, and suppresses growth of both lapatinib-sensitive and lapatinib-resistant cancer cells. a–d The HSF1 inhibitor KRIBB11 suppresses activation of HSF1 (measured by phospho-Ser326) after MG132-induced proteotoxic stress (1 μM, 2.5 h) in lapatinib-sensitive BT474 cells (**a**), suppresses ERBB2 signaling and destabilizes mutp53 in both lapatinib-sensitive BT474 and lapatinib-resistant BT474R cells (**b**), suppresses ERBB2 signaling and HSF1 target Hsp27 in both lapatinib-sensitive 1349 and lapatinib-resistant 125R murine cells (**c**); and induces degradation of mutp53 and Mdm2 in lapatinib-sensitive BT474 cells, which is rescued by the proteasome inhibitor MG132 (**d**). Cells were pre-treated with KRIBB11 (2.5 μM, 24 h) followed by MG132 treatment (1 μM, 2.5 h) (**a**) or simultaneously treated with KRIBB11 (2.5 μM) and MG132 (2.5 μM) for 24 h (**d**). Western blot analyses, GAPDH and Hsc70 served as a loading control. **e, f** The HSF1 inhibitor KRIBB11 suppresses growth of human BT474R (**e**) and mouse 125R (**f**) lapatinib-resistant cells as efficiently as their corresponding lapatinib-sensitive controls, BT474 and 1251, 1252, 1349 cells, respectively. Cells were treated with indicated concentrations of KRIBB11 for 48 h, followed by cell viability assays, which are shown relative to DMSO-treated cells. One representative experiment out of two independent experiments (each performed in triplicate) is shown; NS non-significant

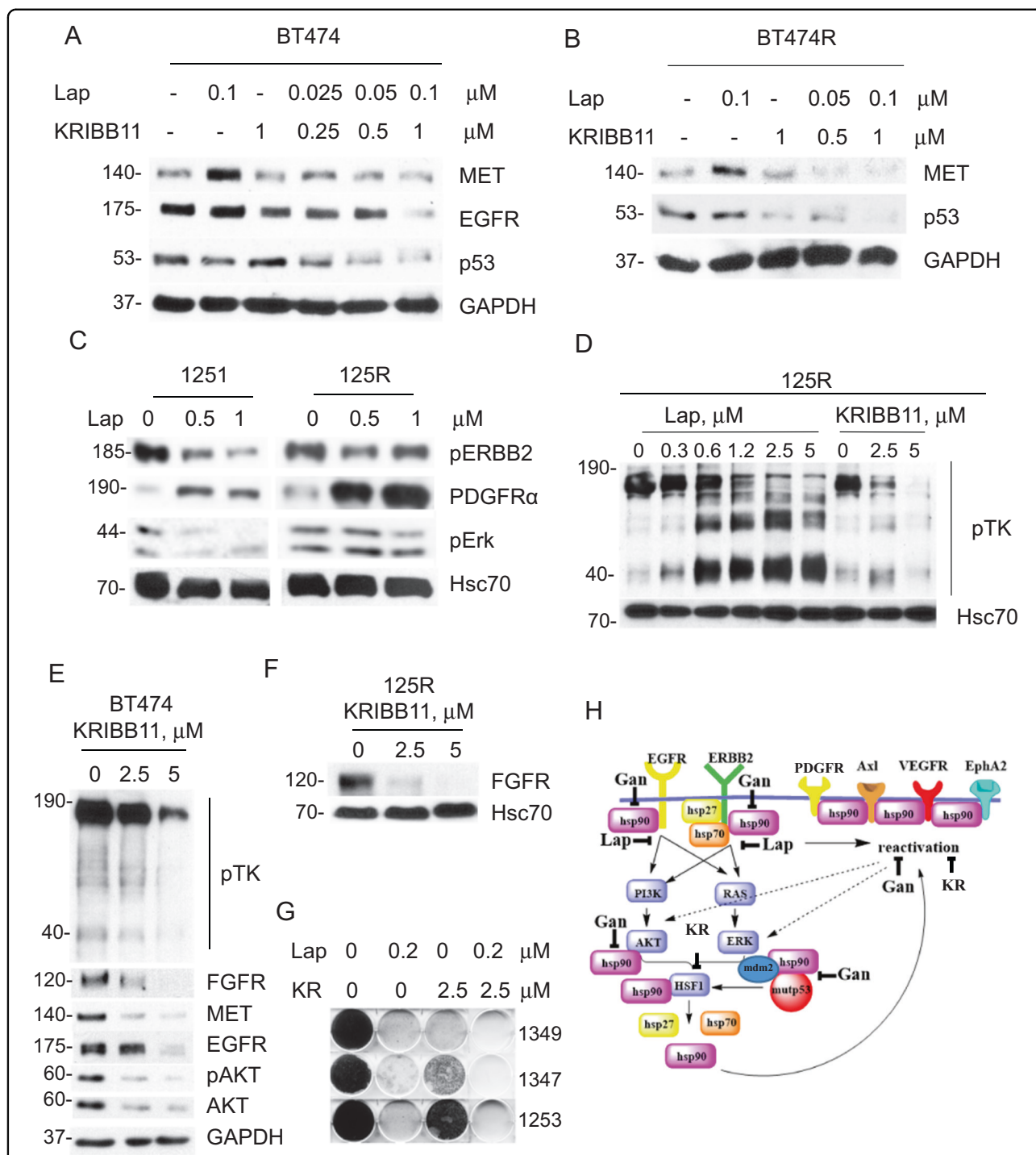


Fig. 6 HSF1 inhibition bypasses lapatinib-induced adaptive signaling and prevents the onset of lapatinib resistance. **a, b** While lapatinib (0.1 μM, 48 h) upregulates MET in both lapatinib-sensitive BT474 (**a**) and lapatinib-resistant BT474R (**b**) cells, HSF1 inhibitor KRIBB11 reverses this effect. Moreover, KRIBB11 synergizes with lapatinib in degradation of EGFR and mutp53 (**a**) and restores responsiveness of mutp53 to lapatinib (**b**). Western blot analyses, GAPDH is a loading control. **c-f** Lapatinib (at indicated concentrations, 48 h) induces PDGFRα in both lapatinib-sensitive 1251 and lapatinib-resistant 125R murine cells (**c**) and induces global kinome activation (measured by phospho-Tyr antibody, pTK) in lapatinib-resistant 125R cells (**d**), KRIBB11 inhibits the global pTK activity and individual kinases in 125R cells (**d, e**), and BT474 cells (**f**). Western blot analysis, Hsc70 and GAPDH are loading controls. **g** KRIBB11 cooperates with lapatinib (at indicated concentrations, for 4 weeks) in suppressing emergence of lapatinib-resistant colonies. Colony formation assay. Representative images out of two technical replicas. **h** The proposed model. ERBB2 signaling mediates HSF1 activation^{4,16}, which is potentiated by mutp53 via a feed-forward loop^{5,15}, thereby upregulating Hsp90 clients including compensatory RTKs and mutp53 itself. Inhibition of ERBB2 by lapatinib leads to inhibition of HSF1 transcriptional activity and therefore decreased Hsp90 and release of Mdm2 from its inhibitory complex with Hsp90^{4,5} and subsequent degradation of mutp53 and Mdm2. KRIBB11 simultaneously inhibits diverse adaptive RTKs, as well as destabilizes potent oncogenic drivers—ERBB2, EGFR, and mutp53

In addition, global assessment of Tyr-phosphorylated proteins—as an indirect readout of overall levels of kinases—revealed an extensive and dose-dependent kinome activation in response to lapatinib in murine 125R cells (Fig. 6d, left), while HSF1 inhibition by KRIBB11 suppressed global kinome activation (Fig. 6d, right) and individual Hsp90 kinase clients, e.g., ERBB2/pERBB2 (Fig. 5c), FGFR (Fig. 6e). To ensure that these effects are specific only to cancer cells, we tested the effect of lapatinib on normal mammary epithelial cells (MECs) isolated from H/H;ERBB2 mice. We found that lapatinib increases total pTK activity only in cancer, but not in MECs (Suppl. Fig. 1), suggesting cancer-specific mechanism of lapatinib-induced kinome reprogramming. This result is consistent with previous study showing high level and activity of HSF1 specifically in human tumor biopsies, but not in normal mammary tissues²⁴. Also, global pTK signal and individual Hsp90 client kinases, e.g., ERBB2, pERBB2 (Fig. 5b), FGFR, MET, EGFR, AKT, and pAKT (Figs. 5b, 6f), were downregulated in human BT474 cells in response to HSF1 inhibition in a dose-dependent manner.

Finally, a colony formation assay showed that while lapatinib-sensitive murine 1349, 1347, and 1253 cells treated with lapatinib or KRIBB11 alone did develop resistant clones, the combinatorial lapatinib/KRIBB11 treatment completely blocked the emergence of resistance (Fig. 6g). Taken together, these results indicate that HSF1 inhibition suppresses global activation of compensatory RTK pathways in response to lapatinib, and therefore can prevent the onset of lapatinib resistance.

Discussion

Although ERBB2-targeted therapies, such as lapatinib, revolutionized management of ERBB2-overexpressing breast cancer, primary and acquired resistance remains a major obstacle for the cure of this deadly disease. Therefore, understanding the mechanisms of lapatinib resistance will greatly facilitate development of successful combinatorial treatments with a durable therapeutic effect. In this study, we utilized an preclinical MMTV-ERBB2;mutp53 mouse model to investigate the mechanism of lapatinib resistance acquired in vivo in ERBB2-positive mammary tumors and to compare them to the resistance mechanisms acquired in vitro.

In both in vivo and in vitro scenarios, we found a robust kinome re-organization in response to ERBB2 inhibition by lapatinib. In agreement with previous studies³, a substantial heterogeneity of adaptive responses was observed in lapatinib-resistant cancer cells, including previously described (Ax1, MET)² and novel upregulated pathways, such as NFGFR, MUSK, VEGFR1, PDGFR α , PDGFR β , EPHA2, and EPHB2 (Fig. 1f). This multifaceted nature of compensatory responses underscores the difficulty of

choosing the most effective drug combination to prevent or overcome lapatinib resistance. In this study we uncovered a common pro-survival mechanism of lapatinib resistance acquired in vivo and in vitro, i.e., an augmented HSF1-mediated heat shock response.

The oncogenic cooperation between ERBB2 and HSF1 was noted previously. Several in vivo studies demonstrated a crucial role of HSF1 in the development of ERBB2-driven breast cancer¹⁰. Not surprisingly, HSF1 protein levels are elevated in 80% of breast cancer cases that are associated with poor prognosis²⁵. Although no clinical studies have directly analyzed the levels of HSF1 or HSPs in lapatinib-resistant tumors, emerging clinical evidence strongly supports our main conclusion. Thus, Phase II clinical trial with an Hsp90 inhibitor tanespimycin (17-AAG) plus trastuzumab (ERBB2-targeted therapy) showed a significant anticancer activity in patients with ERBB2-positive trastuzumab-resistant metastatic breast cancer²⁵. Another a Phase I trial of ganetespib in combination with paclitaxel and trastuzumab in trastuzumab-refractory patients with human ERBB2-positive metastatic breast cancer showed significant clinical benefit of Hsp90 inhibition in triplet therapy²⁶. Altogether, these clinical data strongly support the idea that inhibition of HSF1 and its downstream effectors (e.g., Hsp90) is effective strategy to overcome the resistance to ERBB2-targeted therapies.

Furthermore, we previously demonstrated that HSF1 is an important downstream effector of ERBB2 signaling and that lapatinib inhibits transcriptional activation of HSF1, by suppressing its Ser326 phosphorylation⁵. Most likely, lapatinib affects HSF1 function by inhibiting MAPK and AKT activation, both of which can induce transcriptional phospho-activation of HSF1 at Ser326^{18, 19}. On the other hand, upregulation of compensatory RTKs in lapatinib-resistant cells can induce sustained MAPK and AKT signaling leading to enhanced S326-HSF1 phosphorylation and HSF1 protein stability. In support of this hypothesis we observed higher HSF1 protein and S326-HSF1 level after heat shock in lapatinib-resistant cells (Figs. 1g, h, 2e, f). Our previous study has shown that ERBB2 inhibition in lapatinib-sensitive cells impedes HSF1 activation, leading to the release of Mdm2 from its inhibitory complex with Hsp90 and to mutp53 destabilization⁴ (Figs. 3a, 6h). Strikingly, we now found that in lapatinib-resistant cells, lapatinib fails to modulate the ERBB2–HSF1–mutp53 axis (Fig. 3). Instead, HSF1 is constitutively activated and does not depend on the ERBB2 signaling (Fig. 3c), resulting in a superior tolerance of lapatinib-resistant cells to proteotoxic stress (Fig. 2).

We speculate that in lapatinib-resistant cells, the HSF1 function is restored by activation of adaptive RTKs and their downstream signaling components (Fig. 6h). In turn,

sustained expression of HSPs promotes stability of their clients, adaptive RTKs, thus maintaining continuous HSF1 function (Fig. 6h). Although some elements of this model await further investigation, here we identified HSF1 as an upstream node of the lapatinib resistance mechanisms and demonstrated that its inhibition (i) suppresses global tyrosine-phosphorylation (Fig. 6d, f), (ii) alleviates lapatinib-induced upregulation of specific adaptive RTKs (Fig. 6a, b, c), (iii) synergizes with lapatinib in degradation of mutp53 (Fig. 6a, b), and (iv) prevents development of lapatinib resistance, as measured by appearance of lapatinib-resistant colonies (Fig. 6g).

Importantly, HSF1 inhibition in lapatinib-resistant cells restores mutp53 destabilization in response to lapatinib (Fig. 6b). Highly stabilized mutp53 levels are required for mutp53 oncogenic gain-of-function¹⁷, and mutp53 genetic and pharmacological ablation significantly suppresses malignant phenotypes in mutp53-carrying cancers¹⁷. Therefore, identification of compounds targeting mutp53 for degradation has a major translational impact for ERBB2-positive breast cancer therapy, given the high frequency of p53 mutations in this breast cancer subtype.

In sum, we showed that pharmacological inhibition of HSF1 simultaneously inhibits diverse adaptive responses endowing lapatinib resistance, as well as destabilizes potent oncogenic drivers of ERBB2-positive breast cancer, such as ERBB2, EGFR, and mutp53. Thus, targeting HSF1 and opens up a new therapeutic possibility for the clinical application of HSF1 inhibitors to prevent and/or delay onset of lapatinib resistance with a potential of the instant clinical translation.

Materials and methods

Human cancer cells

Human ERBB2-positive breast cancer cell line BT474 carrying E285K *TP53* mutation was purchased from ATCC in 2013. ATCC verifies cell's identity with short tandem repeat analysis. To generate lapatinib-resistant BT474R cell line, parental BT474 cells were cultivated in the presence of increasing concentrations (100–300 nM) of lapatinib for 6 months, as previously described³. No further cell's identity verification was performed. Unless indicated otherwise, lapatinib-resistant BT474R cells were routinely maintained in the presence of 300 nM lapatinib. Where shown, cells were treated with indicated concentrations of lapatinib (L-4899, LC Lab), MG132 (M7449, Sigma), ganetespib (STA-9090, Synta Pharmaceuticals, Lexington, MA, USA), KRIBB11 (385570, Calbiochem, Billerica, MA, USA). All cell viability assays were done using standard clonogenicity assays and CellTiter-Blue Cell Viability Assay (Promega, 96-well format with 5000 cells/well seeded 24 h prior). Prior to the CTB assay (Fig. 1a), cells were maintained in lapatinib-free media for 3 days. Cells were treated with drugs for 48 h, unless

indicated otherwise, with drug concentrations as shown. Fluorescence was detected by SPECTRAmax M2 (Molecular Devices).

Animals

MMTV-ERBB2 mice harboring activated ERBB2 were from Jackson Labs (strain FVBN-Tg(MMTV-ERBB2) NK1Mul/J). mutp53 R172H mice were a gift from G. Lozano²⁷. Generation of R172H/+;ERBB2 compound mice was described previously¹⁵. Eight weeks old R172H/+;ERBB2 littermate females, all on C57Bl6/J:FVB/N 50:50 background, were treated with vehicle (18% Cremophor/3.6% dextrose) or lapatinib (75 mg/kg three times a week) by oral gavage lifelong. When lapatinib-treated tumors acquired lapatinib resistance, animals were treated with either vehicle, lapatinib alone, or lapatinib with ganetespib, as described in the text. Ganetespib was prepared as previously described¹⁷ and injected into the tail vein at 50 mg/kg once a week. At endpoint (tumor size ~3.5 cm³) mice were sacrificed and some of lapatinib only treated tumors were used to establish cell cultures. Mice were treated according to the guidelines approved by the Stony Brook University Institutional Animal Care and Use Committee.

Establishing primary mammary tumor cell cultures

Mammary tumors were dissected from mice, rinsed three times in PBS, and sequentially digested with collagenase/hyaluronidase (37°C, 2 h), 0.05% Trypsin, DNase I, and Dispase (Stem Cell Technology). The ensuing cell suspensions were treated with red blood cell lysis buffer, rinsed with PBS, resuspended in Opti-MEM medium (Gibco) and passed through a 40 µm mesh to remove cell chunks. Cells were plated on gelatin-coated plates and grown in CnT-BM1 medium (Cell-N-Tec). Unless indicated otherwise, lapatinib-resistant 125R cells derived from a lapatinib-resistant mammary tumor were routinely maintained in the presence of 300 nM of lapatinib. Heterozygous mutant p53 R172H/+ status was verified and confirmed by using genotyping primers²⁷ in all established mouse cell lines.

Immunoblot analysis and kinome arrays

For immunoblots, cell lysates with equal total protein content (2–20 µg) were blotted with antibodies to p53 (FL393), Mdm2, GAPDH, Hsc70 (all from Santa Cruz Biotechnology); Erk1, pErk1/2 (T202/Y204), EGFR, pEGFR (Y845), ERBB2, pERBB2 (Y1221/1222 and pY1248), MET, cleaved PARP, PDGFRα, PDGFRβ, FGFR, AKT, pAKT MdmX, pTK (all from Cell Signaling); HSF1, pHSF1 (S326), Hsp90, Hsp70, Hsp27 (all from Enzo Life Sciences Inc., Farmingdale, NY). All Western blots were repeated at least two times. The phospho-RTK array on primary mammary tumor cells was performed according

to the manufacturer's protocol (Mouse Phospho-RTK Array Kit, R&D Systems).

Statistical analysis

Unpaired two-tailed Student's *t*-test was used to calculate statistical significance (*p*-value). Kaplan–Meier analysis and log rank statistics were used to compare animal survival. All experiments were repeated in at least two biological replicas with three technical replicas each, unless indicated otherwise.

Acknowledgements

This work was supported by the Department of Defense grant W81XWH-16-1-0448 (BC151569) and the Carol Baldwin Breast Cancer Research Fund to N.M. and NIH/NCI grant K22CA190653-01A1 to E.M.A.

Conflict of interest

The authors declare that they have no conflict of interest.

Publisher's note

Springer Nature remains neutral with regard to jurisdictional claims in published maps and institutional affiliations.

Supplementary Information accompanies this paper at (<https://doi.org/10.1038/s41419-018-0691-x>).

Received: 29 January 2018 Revised: 6 May 2018 Accepted: 7 May 2018
Published online: 24 May 2018

References

- Yarden, Y. & Pines, G. The ERBB network: at last, cancer therapy meets systems biology. *Nat. Rev. Cancer* **12**, 553–563 (2012).
- D'Amato, V. et al. Mechanisms of lapatinib resistance in HER2-driven breast cancer. *Cancer Treat. Rev.* **41**, 877–883 (2015).
- Stuhlmiller, T. J. et al. Inhibition of lapatinib-induced kinome reprogramming in ERBB2-positive breast cancer by targeting BET family bromodomains. *Cell Rep.* **11**, 390–404 (2015).
- Li, D. & Marchenko, N. D. ErbB2 inhibition by lapatinib promotes degradation of mutant p53 protein in cancer cells. *Oncotarget* **8**, 5823–5833 (2017).
- Li, D., Yallowitz, A., Ozog, L. & Marchenko, N. A gain-of-function mutant p53-HSF1 feed forward circuit governs adaptation of cancer cells to proteotoxic stress. *Cell Death Dis.* **5**, e1194 (2014).
- Alexandrova, E. M. & Marchenko, N. D. Mutant p53-heat shock response oncogenic cooperation: a new mechanism of cancer cell survival. *Front. Endocrinol.* **6**, 53 (2015).
- Ciocca, D. R., Arrigo, A. P. & Calderwood, S. K. Heat shock proteins and heat shock factor 1 in carcinogenesis and tumor development: an update. *Arch. Toxicol.* **87**, 19–48 (2013).
- Dai, C., Whitesell, L., Rogers, A. B. & Lindquist, S. Heat shock factor 1 is a powerful multifaceted modifier of carcinogenesis. *Cell* **130**, 1005–1018 (2007).
- Mendillo, M. L. et al. HSF1 drives a transcriptional program distinct from heat shock to support highly malignant human cancers. *Cell* **150**, 549–562 (2012).
- Xi, C., Hu, Y., Buckhaults, P., Moskophidis, D. & Mivechi, N. F. Heat shock factor Hsf1 cooperates with ErbB2 (Her2/Neu) protein to promote mammary tumorigenesis and metastasis. *J. Biol. Chem.* **287**, 35646–35657 (2012).
- Powers, M. V., Clarke, P. A. & Workman, P. Dual targeting of HSC70 and HSP72 inhibits HSP90 function and induces tumor-specific apoptosis. *Cancer Cell.* **14**, 250–262 (2008).
- Cancer Genome Atlas N. Comprehensive molecular portraits of human breast tumours. *Nature* **490**, 61–70 (2012).
- Rahko, E., Blanco, G., Soini, Y., Bloigu, R. & Jukkola, A. A mutant TP53 gene status is associated with a poor prognosis and anthracycline-resistance in breast cancer patients. *Eur. J. Cancer* **39**, 447–453 (2003).
- Yallowitz, A. R. et al. Mutant p53 amplifies epidermal growth factor receptor family signaling to promote mammary tumorigenesis. *Mol. Cancer Res.* **13**, 743–754 (2015).
- Schulz, R. et al. HER2/ErbB2 activates HSF1 and thereby controls HSP90 clients including MIF in HER2-overexpressing breast cancer. *Cell Death Dis.* **5**, e980 (2014).
- Alexandrova, E. M. et al. Improving survival by exploiting tumour dependence on stabilized mutant p53 for treatment. *Nature* **523**, 352–356 (2015).
- Dai, C. et al. Loss of tumor suppressor NF1 activates HSF1 to promote carcinogenesis. *J. Clin. Invest.* **122**, 3742–3754 (2012).
- Carpenter, R. L., Paw, I., Dewhirst, M. W. & Lo, H. W. Akt phosphorylates and activates HSF-1 independent of heat shock, leading to Slug overexpression and epithelial-mesenchymal transition (EMT) of HER2-overexpressing breast cancer cells. *Oncogene* **34**, 546–557 (2015).
- Powers, M. V. & Workman, P. Targeting of multiple signalling pathways by heat shock protein 90 molecular chaperone inhibitors. *Endocr. Relat. Cancer* **13**, S125–S135 (2006).
- Friedland, J. C. et al. Targeted inhibition of Hsp90 by ganetespib is effective across a broad spectrum of breast cancer subtypes. *Invest. New Drugs* **32**, 14–24 (2014).
- Yoon, Y. J. et al. KRIBB11 inhibits HSP70 synthesis through inhibition of heat shock factor 1 function by impairing the recruitment of positive transcription elongation factor b to the hsp70 promoter. *J. Biol. Chem.* **286**, 1737–1747 (2011).
- Choi, Y. J. et al. AUY922 effectively overcomes MET- and AXL-mediated resistance to EGFR-TKI in lung cancer cells. *PLoS ONE* **10**, e0119832 (2015).
- Matei, D. et al. The platelet-derived growth factor receptor alpha is destabilized by geldanamycins in cancer cells. *J. Biol. Chem.* **282**, 445–453 (2007).
- Santagata, S. et al. High levels of nuclear heat-shock factor 1 (HSF1) are associated with poor prognosis in breast cancer. *Proc. Natl Acad. Sci. USA* **108**, 18378–18383 (2011).
- Modi, S. et al. HSP90 inhibition is effective in breast cancer: a phase II trial of tanespimycin (17-AAG) plus trastuzumab in patients with HER2-positive metastatic breast cancer progressing on trastuzumab. *Clin. Cancer Res.* **17**, 5132–5139 (2011).
- Jhaveri, K. et al. A phase I trial of ganetespib in combination with paclitaxel and trastuzumab in patients with human epidermal growth factor receptor-2 (HER2)-positive metastatic breast cancer. *Breast Cancer Res.* **19**, 89 (2017).
- Lang, G. A. et al. Gain of function of a p53 hot spot mutation in a mouse model of Li-Fraumeni syndrome. *Cell* **119**, 861–872 (2004).